UNIVERSITY of WASHINGTON

AIAA/Cessna/Raytheon
Design/Build/Fly
2014 - 2015

WOOFfle Baller

Table of Contents

1. Executive Summary **2**

2. Management Summary **3**

2.1 Team Organization 3

2.2 Milestone Flow Chart 4

3. Conceptual Design **5**

3.1 Mission Requirement and Constraints 5

3.2 Configuration Selection 13

4. Preliminary Design **21**

4.1 Analysis Methodology 21

4.2 Mission Model 22

4.3 Design and Sizing Trades 23

4.4 Lift, Drag, and Stability Characteristics 31

5. Detailed Design **34**

5.1 Dimensional Parameters 34

5.2 Structure Characteristics and Capabilities 35

5.3 Subsystem Design 37

5.4 Weight and Balance 39

5.5 Performance Parameters 40

5.6 Drawing Packages 41

6. Manufacturing Plan **46**

6.1 Manufacturing Schedule 46

6.2 Material Selection 46

6.3 Major Component Manufacturing Process 47

7. Testing Plan **50**

7.1 Subsystem Test 50

7.2 Flight Test 52

7.3 Testing Schedule 53

8. Performance Results **54**

8.1 Subsystem Test Results 54

8.2 Flight and Mission Performance 55

References **56**

1. Executive Summary

The following report serves to document and analyze Design, Build, Fly at the University of Washington's design, construction, and performance results that led to the final design of the aircraft built for the 2014-2015 AIAA Design/Build/Fly Competition.

The missions in this year's competition model an airdrop scenario, specifically the kind that a military aircraft might complete in delivering supplies to an isolated area. The missions include a ground mission, in which the payloads used later for missions 1 and 2 must be quickly loaded and unloaded from the aircraft. The ground mission tests the ability of the aircraft to securely hold all payloads while still maintaining easy access to these payloads. The first flight mission, a ferry flight, tests the speed and handling capabilities of the aircraft. The second flight mission is a sensor package transport mission, during which the aircraft must fly three laps with a heavy payload in the shortest amount of time possible. Success in this mission requires the aircraft to be able to generate high levels of lift while still maintaining speed and good handling characteristics. The final flight mission is the sensor drop mission. It is during this mission that the aircraft must be able to accurately drop sensors (modeled by plastic balls) over a drop zone, once per lap. In order for this mission to be a success, the aircraft should be equipped with a well-designed dropping mechanism with the ability to hold and release the plastic balls on command. The intent of this mission is to be able to drop supplies within a preset range for the intended recipients.

Through careful scoring sensitivity analysis, it was determined that the most important design points were minimizing the weight of the aircraft and reducing the number of servos, all while maximizing the accommodation for plastic balls and maintaining a high velocity. By using foam as the main structural component of the aircraft, the weight of the aircraft was drastically reduced. The velocity of the aircraft was maximized by increasing the motor's thrust and minimizing the drag caused by the plastic balls, mainly by lining them up along the length of the fuselage. The drag was further reduced by selecting a high lift-to-drag ratio wing airfoil and an airfoil-shaped fuselage. The chosen aircraft design also minimized the number of servos used by eliminating the ailerons and adopting a simple-structured dropping mechanism which shares a servo with the elevator. This reduction in servos directly improved the aircraft's expected score.

Currently, the design model has a 2.6 lb. empty weight, a maximum velocity of 30 m/s, with only two servos and one speed controller on board. The fuselage is airfoil-shaped and can accommodate the dimensions of the payload for the second flight mission. The aircraft was successfully tested holding five plastic balls externally and has complete control of the release timing. The aircraft model was able to complete eight laps in four minutes and fly three laps with the maximum payload in 2.15 minutes. Further optimization will take place prior to the competition.

Thus, a lighter aircraft that possibly carries more plastic balls and has better performance characteristics will be presented at the competition by Design, Build, Fly at the University of Washington.

Through careful analysis of the aircraft design and extensive testing, the University of Washington will be competing for first place in the 2014-2015 AIAA Design/Build/Fly Competition.

2. Management Summary

Design, Build, Fly at the University of Washington is composed of 24 dedicated members: 3 freshmen, 6 sophomores, 14 juniors, and 1 senior. The UW team used Scrum methodology to organize and collaborate with all members. Specific goals in production were broken down into specific tasks which were set to be completed by the end of each month. Using an online system, members were delegated these specific tasks. At the end of each month, an all-hands meeting was held to discuss the tasks that were attempted and improvements that needed to be made in order for the tasks to be considered complete.

2.1 Team Organization

Design, Build, Fly at the University of Washington is composed of four divisions: Administrative, Design, Construction, and Documentation. Each division has leaders responsible for managing task delegation and timeline adherence. The Administrative team is in charge of opening communication between groups, organizing sponsorships and funding, and ensuring the entire DBF team satisfies specific AIAA competition guidelines. The Design team is in charge of designing an aircraft that both fulfills the competition's specifications, and is optimized to achieve the maximum score. The Construction team is responsible for sourcing materials and building the aircraft to satisfy the design. The Design team works closely with the Construction team to check if the design can be fabricated or machined with the tools and materials that are available. Once the aircraft is assembled, Design and Construction members work together in testing and modifying the aircraft. The Documentation team is tasked with recording the entire project's process and compiling all information into a formal report to be submitted for the competition. The individuals in the Documentation team must work closely with each of the other teams to document all the processes and decisions made throughout the duration of the project. The organizational structure of the DBF leadership team is shown below in Figure 2.1.

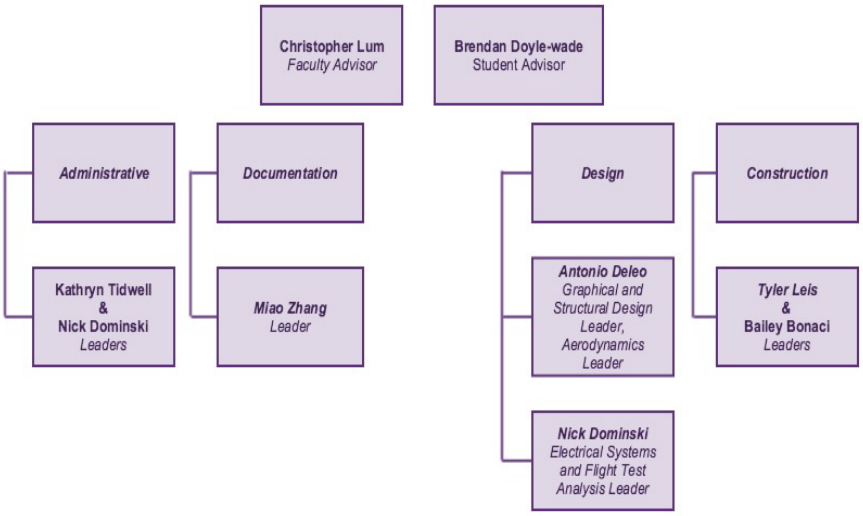

Figure 2.1: Leadership structure for Design, Build, Fly at the University of Washington

2.2 Milestone Flow Chart

The milestone chart, shown below in Figure 2.2, displays the schedule for aircraft design, construction, and testing. The Administrative team and team leaders responsible for each individual project cooperated to ensure time adherence. Both planned and actual progress are shown in the flow chart.

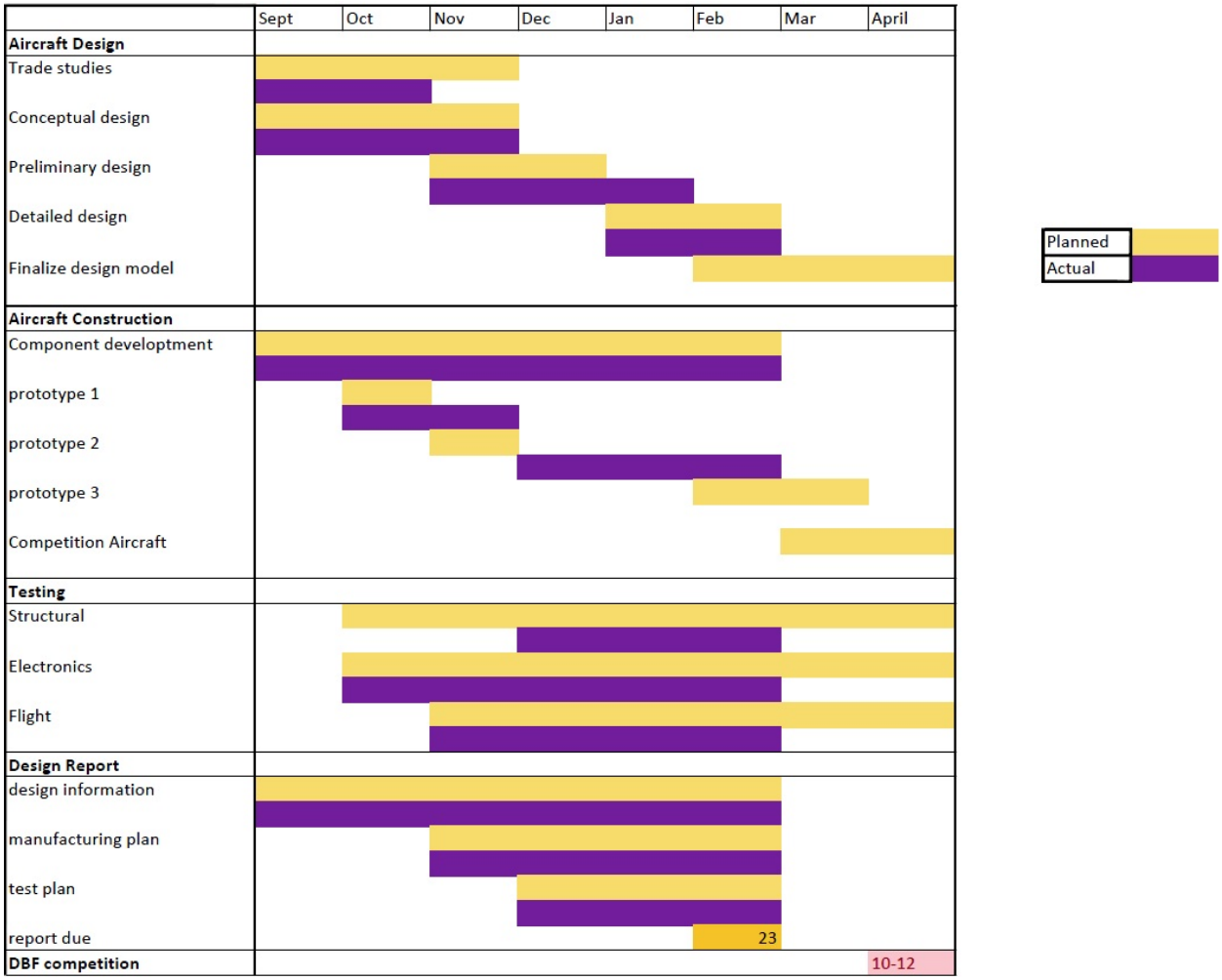

Figure 2.2: Milestone flow chart

3. Conceptual Design

3.1 Mission Requirements and Constraints

The 2015 American Institute of Aeronautics and Astronautics (AIAA) Design/Build/Fly (DBF) Competition comprises four aircraft missions: one ground mission, three flight missions. The Ground Mission may be completed at any time the flight line is open, while the three Flight Missions must be flown in order. Each flight mission must begin with takeoff within the prescribed length of runway and conclude with a successful landing to receive a score. The team is allocated 5 minutes to load the payload and run a check for the aircrafts systems functionality. After this time, work is no longer allowed on the aircraft. Only three team members are allowed within the staging box: the assembly crew member, pilot and pilot assistant. After the three flight missions are complete and

have been scored, the team can opt to attempt a single re-flight of each mission. The larger of the two trials scores will count towards the total mission score. The layout is a 1000-ft. course with two 180º turns on each end and one 360º turn halfway through the course as can be seen in Figure 3.1. The orientation (direction) of the flight course will be adjusted based on the prevailing winds as determined by the Flight Line Judge.

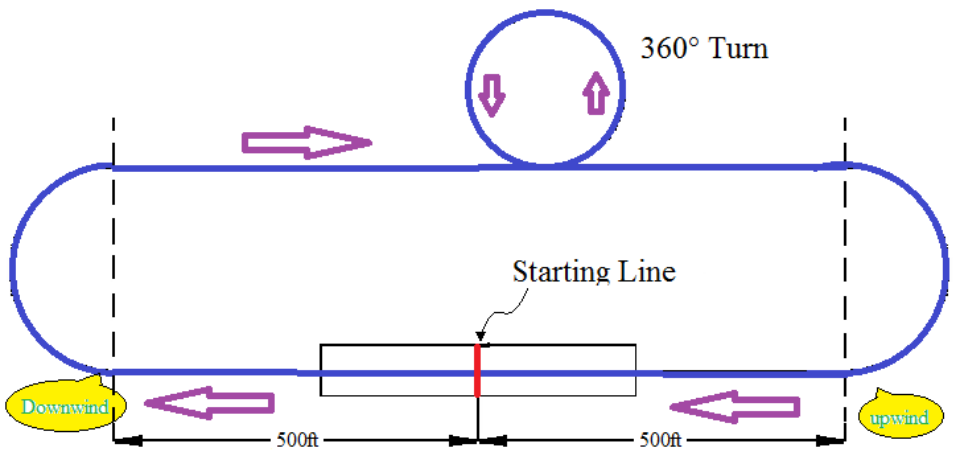

Figure 3.1: Course layout (downwind and upwind marker may be reversed)

The UW team has analyzed and discussed the contest rule of the 2015 AIAA DBF Competition, and summarized crucial constraints, as well as notable design flexibility, which composes the criterion for our design.

Contest constraints

- All vehicles will undergo a safety inspection by a designated contest safety inspector prior to being allowed to make any competition flight
- Aircraft will use ground rolling take-off and landing
- Takeoff field length will be limited to 60 ft.
- No structure/components may be dropped from the aircraft during flight.
- All energy for take-off must come from the on-board propulsion battery pack(s)
- Batteries may not be changed or charged during a flight mission attempt.
- All payloads must be secured sufficiently to assure safe flight without possible variation of aircraft CG outside of design limits during flight.

Aircraft constraints

- The aircraft must be designed to fly all of the three flight missions

- The aircraft may be of any configuration except rotary wing or lighter-than-air.
- Must be propeller driven and electric powered with an unmodified over-the-counter model electric motor. May use multiple motors and/or propellers. May be direct drive or with gear or belt reduction.
- Each aircraft will use a commercially produced propeller/blades. Must use a commercially available propeller hub/pitch mechanism
- Must use over the counter NiCad or NiMH batteries
- Radio Rx and servos MUST be on a separate battery pack with the propulsion system.
- Battery pack(s) maximum weight limit is 2.0 lb.

Design flexibility

- Propeller diameter/pitch are adjustable for each flight attempt.
- Motors may be any commercial brush or brushless electric motor.

3.1.1 Scoring Summary

The total score for the 2015 AIAA DBF Competition is given by Equation 3.1.

$$\text{Total Score} = \frac{\text{Written Report Score} \times \text{Total Mission Score}}{\text{RAC}} \tag{3.1}$$

The Written Report Score is scored on a 100-point scale and is based on the quality of the report. The Total Mission Score is a function of the Ground Score, GS, and the Flight Score, FS. The Total Mission Score is given by Equation 3.2.

$$\text{Total Mission Score} = \text{GS} \times \text{FS} \tag{3.2}$$

The Ground Score, GS, is based off of a grounded flight mission and is further described in Section 3.1.2. The Flight Score, FS, is the sum of the three individual flight mission scores and is given by Equation 3.3.

$$\text{FS} = \text{M1} + \text{M2} + \text{M3} \tag{3.3}$$

M1, M2, and M3 describe the scores of Flight Missions 1, 2 and 3 respectively. The Mission Scores are explained further in Section 3.1.2.

RAC is the Rated Aircraft Cost. RAC is a function of the Empty Weight of the aircraft, EW, and the Number of Servos used, N_{Servos}. Equation 3.4 defines the RAC.

$$\text{RAC} = \text{EW} \times N_{Servos} \tag{3.4}$$

The Empty Weight, EW, will be measured after each successful scoring flight. The final value for EW will be taken according to Equation 3.5 as the maximum empty weight over all three of the flight missions.

$$\text{EW} = \text{Max}(\text{EW1}, \text{EW2}, \text{EW3}) \tag{3.5}$$

A servo is defined as any mechanical or electrical device used to control the airplane or the payload release mechanism. The Number of Servos used is the sum of all of the servos used throughout the missions, which is the value N_{Servos} in Equation 3.4.

3.1.2 Mission Description

Ground Mission: Payload Loading Time

The objective of the Payload Loading Time Mission is to quickly secure a payload to the aircraft. The time taken to secure the payloads for both Flight Missions 2 and 3 will be recorded. The mission starts with an empty aircraft with all hatches closed. Time starts when the crew begins loading the Mission 2 payload and time is paused when the crew leaves the loading area. During the pause, the payload is verified as secure for flight. Time is then restarted, and the crew removes the Mission 2 payload and loads the Mission 3 payload. Mission 3 payload should contain the maximum number of plastic balls declared during Tech Inspection. Once the crew leaves the loading area, the time is stopped and recorded, and verification of secure payload is executed. The mission must be completed in less than five minutes to be considered complete. Equation 3.6 describes the scoring for GS.

$$GS = \begin{cases} t_{fastest\ GM} / t_{UWGM} & \text{upon sucessful completion} \\ 0.2 & \text{upon failure to complete} \end{cases} \tag{3.6}$$

Where $t_{fastest\ GM}$, is the fastest successful time amongst all teams to complete the Ground Mission and t_{UWGM} is the time recorded for the completion of the Ground Mission time for UW.

Flight Mission 1: Ferry Flight

The objective of the Ferry Flight mission is to fly as many complete laps as possible within four minutes after taking off within the 60 ft. field length. Timing begins when the throttle is advanced for the first take-off or attempted take-off. One lap is counted as the aircraft flies over the start/finish line in the air. There is no payload installed for this mission. The score for Flight Mission 1, M1, is given by Equation 3.7.

$$M1 = 2 \times \frac{N_{Laps,M1,UW}}{N_{Laps,M1,Max}} \tag{3.7}$$

A successful landing must be executed for this mission to receive a score.

Flight Mission 2: Sensor Package Transport Mission

The objective of the Sensor Package Transport Mission is to fly a heavy payload three laps around the flight course in the smallest interval of time possible. The Sensor Package is comprised of one stack of three standard 2 x 6 wooden pine boards that are 10'' long with a total nominal weight of 5 lb. The boards will be fastened together to form one single block. The payload is depicted below in Fig 3.2.

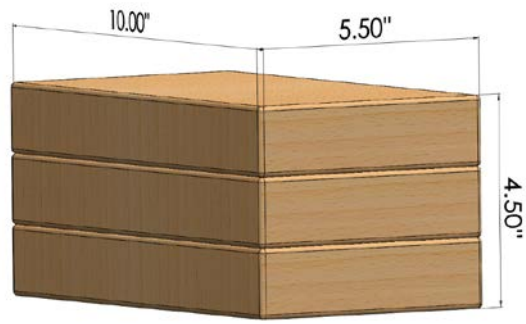

Figure 3.2: Mission 2 payload

The payload is to be properly secured internally to the aircraft, which is defined as completely enclosed by the structure and skin of the aircraft. No part of the payload may be exposed to the free stream air. Time begins once the throttle is advanced for take-off or attempted take-off. Time finishes recording once the aircraft passes over the finish line (in the air) after completion of the third lap of the flight course. Time is measured in seconds. Equation 3.8 describes the scoring for Flight Mission 2, M2.

$$M2 = 4 \times \frac{t_{M2,\,fastest}}{t_{M2,UW}} \tag{3.8}$$

The variable $t_{M2,\,fastest}$, is defined as the fastest recorded time for Flight Mission 2 amongst all teams and $t_{M2,UW}$, is defined as the recorded time for Flight Mission 2 for UW. A successful landing must be executed for this mission to receive a score.

Flight Mission 3: Sensor Drop Mission

The objective of the Sensor Drop Mission is to accurately drop a payload within the bounds of a specified drop zone. The payload for Flight Mission 3 is a team-selected number of Champro 12'' Plastic Balls. Payloads and supporting equipment for mission 3 must be secured external to the aircraft configuration of mission 1 and 2. The aircraft will take off within the prescribed field length. After completing a lap, the aircraft will remotely drop a single ball over the drop zone. The drop zone is described in Figure 3.3.

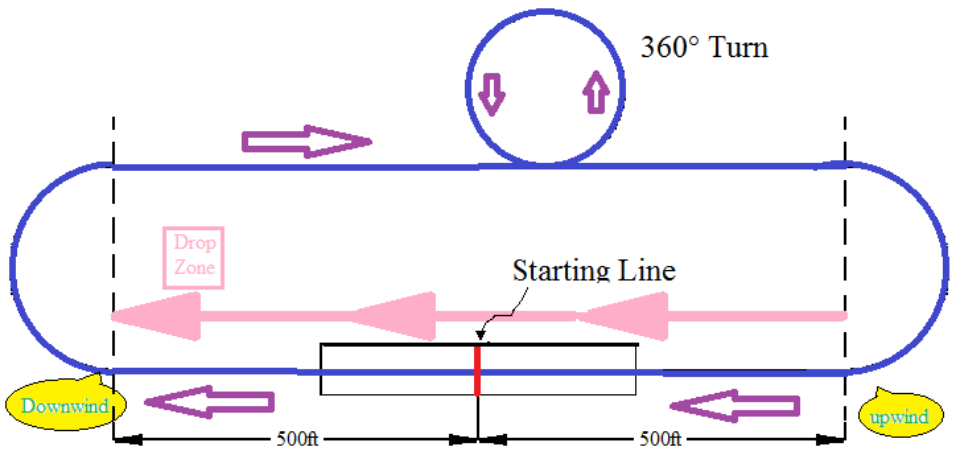

Figure 3.3: Drop zone for flight mission 3 (downwind and upwind marker may be reversed)

A lap will only be counted if a single ball is dropped within the drop zone. If multiple drops occur during the same lap, the lap is invalidated. The score for Flight Mission 3, M3, is given by Equation 3.9.

$$M3 = 6 \times \frac{N_{Laps,M3,UW}}{N_{Laps,M3,Max}} \tag{3.9}$$

The variable $N_{Laps,M3,UW}$, is defined as the number of laps UW completes for Flight Mission 3 and $N_{Laps,M3,Max}$ is defined as the maximum number of laps achieved among all teams during the competition. A successful landing must be executed for this mission to receive a score.

3.1.3 Design Requirement

Sensitivity Analysis

To determine which factors of the aircraft and missions would have the greatest effect on the total score, a sensitivity analysis was conducted. By assigning an average score to use as a base value, percent changes were made to different scoring parameters and the resulting change in the total score was calculated in each case. Using MATLAB, these sensitivity relationships were plotted in Figure 3.1.

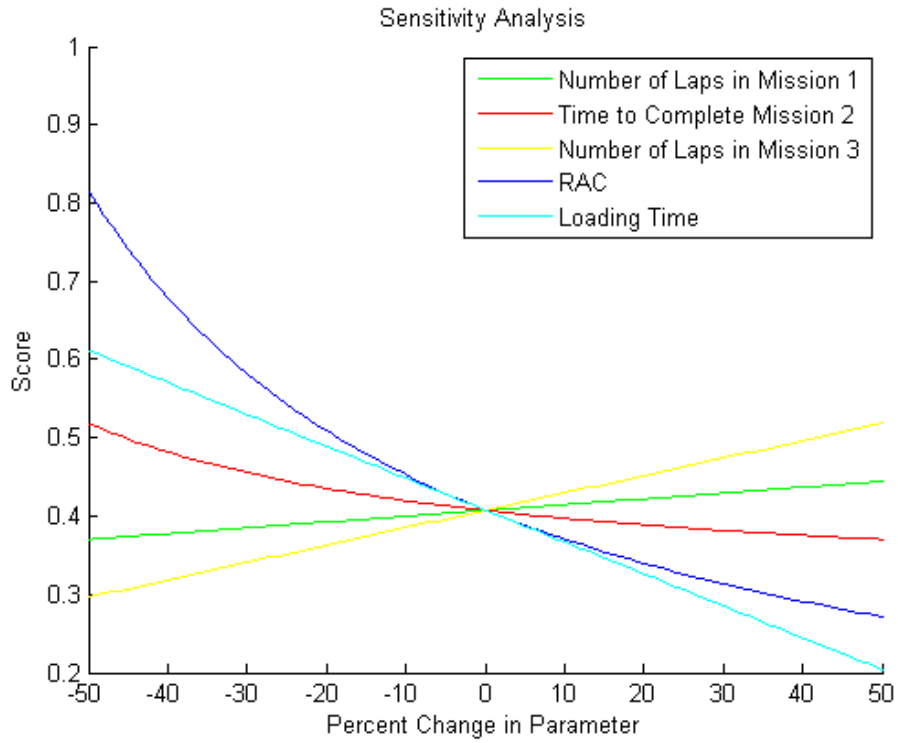

Figure 3.4: Percentage change in total score vs. percentage change in scoring variable

The parameters with the steepest curves have the largest effect on the total score for a given percent change. Taking this into account, it can be seen from Figure 3.1 that the aircraft RAC and the time to load the aircraft during the ground mission play the most significant role in the total score. Of the three flight missions, Mission 3's score has the largest effect on the total score; Mission 1, with the least steep slope, has the smallest effect. This analysis indicated that the weight of the aircraft and number of servos are of higher priority than the maximum speed.

Feature Analysis

In order to excel in the competition, a careful analysis of the mission requirements must take place. Each mission requires different design elements from the aircraft. In this section, the design requirements of each mission will be examined.

For the ground mission, the aircraft must have efficient and secure payload stabilization. Crewmembers must be able to quickly secure payloads for Missions 2 and 3. The storage volume inside the aircraft must also be made easily accessible to the crewmembers and the payload needs to be quickly securable. Payload areas include the main storage volume within the fuselage and the targeting payload area underneath the fuselage.

For the ferry flight mission there are two main design requirements. The aircraft must have a high maximum velocity and sufficient in-air maneuverability. In order to maintain a high maximum velocity, the aircraft must be low in weight, have high thrust capabilities, and low drag. In order to provide in air maneuverability, the aircraft must have high lift and there must be good control and deflection range of manipulated surfaces.

For the sensor package transport mission, the size and lifting capabilities of the aircraft are the most important features. The fuselage must be large enough to house the sensor package, the power system must be capable of giving the aircraft enough velocity for flight, and the wings must produce enough lift. The structure of the aircraft must be able to tolerate the forces introduced by the substantial weight of the sensor package. An ideal dropping mechanism that will be beneficial for high performance would be able to hold and drop the plastic balls on command without adding excess weight. Simple structures are preferred as complex structures tend to add more weight on the aircraft and have a higher chance of failure.

For the sensor drop mission, the structure holding the sensors must be able to tolerate the aerodynamic forces applied in flight. Due to the requirement that only one sensor can be dropped for each lap, the aircraft must also have precise control over when each individual sensor is dropped.

Scoring demands that the aircraft have a low RAC. In order to accomplish this, the aircraft must be lightweight and have a low number of servos.

Design Requirement Summary

Each mission requires a different set of design requirements. Some of these requirements interfere with design requirements of other missions. Based on the scoring analysis, the final design elements will be chosen. The requirements that have a minimal impact on total score were less emphasized in the final design configuration.

As shown in the sensitivity analysis, the number of laps in mission 3, which requires the aircraft to carry same number of plastic balls, has the largest effect on the final flight score. However, carrying more plastic balls requires a larger aerodynamic profile of the airframe, which will increase the drag and slow down the aircraft for missions 1 and 2. Moreover, more laps also requires more energy from the battery packs, and implies added battery weight. Therefore, the optimization of the number of plastic balls must be performed.

3.2 Configuration Selection

3.2.1 Propulsion System Selection

In previous years, the competition has enforced a current limit via a required fuse in every closed battery-motor circuit. This is not the case in the 2015 competition. The only enforced limit regarding the power system is a 2lb limit on the battery weight. This rule change has a large effect on the decision process for selecting a motor configuration. In addition to this rule change, each ESC used to control a motor was also counted as a servo actuator. This meant that our initial attitude was to use only a single motor, and the resulting trade study was conducted only to explore the possibility of any great benefit that might possibly be presented in a multi-motor situation.

The two motor configurations considered are shown below in Figures 3.6 and 3.7. A pusher motor setup was immediately disqualified as this would create a propeller damage hazard during the sensor dropping mission.

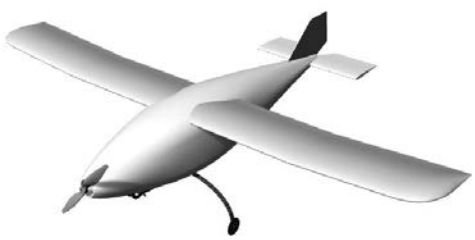

Figure 3.6: Single tractor

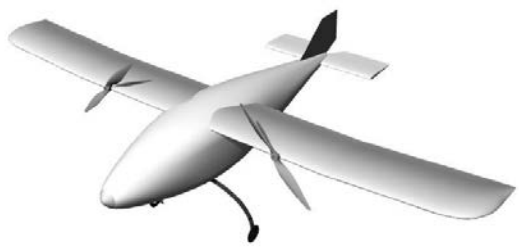

Figure 3.7: Twin tractor

The goal of the propulsion system selection is to find the optimum motor configuration for high thrust, low weight, and efficiency. A trade study was conducted to analyze these parameters for each configuration. The 'single tractor' configuration was assigned a 0 for each parameter as a baseline.

Table 3.2: Propulsion system trade study results

	Structural	Efficiency	Weight	Aerodynamics	Total
Single Tractor	0	0	0	0	0
Twin Tractor	-1	-1	-1	1	-2

For the structural category the twin tractor configuration received a '-1' score due to the added structural complexity needed to mount each motor on the wings. This, combined with the additional electronic speed controller required, is also the reason the twin tractor configuration received a '-1' score for the weight category. For the efficiency category the twin tractor configuration received a

‘-1’ score due to the lost efficiency in extra material weight and loss in electrical efficiency due to the necessity for two electronic speed controllers and battery packs. The twin tractor configuration received a ‘+1’ in the aerodynamics category due to the accelerated air, or prop wash, flowing over the wings aft of the propellers. The total score for the single tractor configuration was 0 while for the twin tractor it was -2. The single tractor configuration was chosen as final configuration for the competition.

3.2.2 Empennage Selection

In order to select a preliminary empennage, a trade study was performed to weigh the benefits of certain features. The team considered four configurations: conventional (Figure 3.8), H-tail (Figure 3.89), T-tail (Figure 3.10), and V-tail (Figure 3.11). The conventional empennage was set as the reference configuration and was thus given a score of zero for all sections.

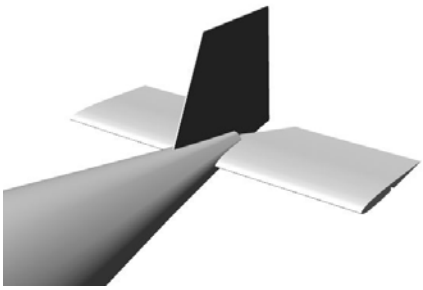

Figure 3.8: Conventional

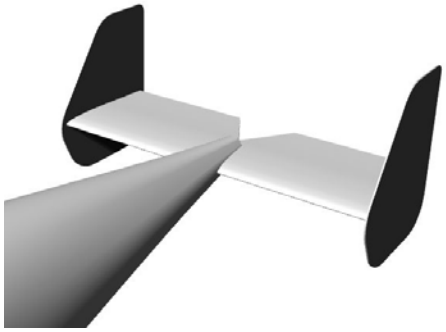

Figure 3.9: H-tail

Figure 3.10: T-tail

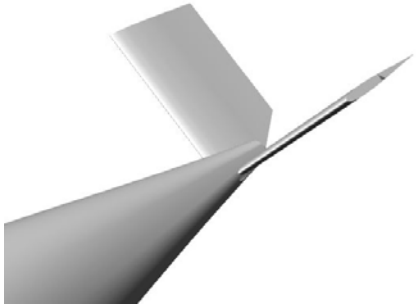

Figure 3.11: V-tail

To assign scores for the number of servos required, each additional servo required (with respect to the conventional configuration’s two servos) corresponded to -1 point. Because the number of servos required directly affects the flight score, these point values were assigned a multiplier of 2 to weigh the effect more heavily. The V-tail can be constructed with only 2 servos and thus received

a score of 0. The T-tail can also be constructed with only 2 servos and thus received a score of 0. The conventional tail without a rudder only requires 1 servo and thus received a score of +1.

In order to determine weight scoring, the structural implications of each empennage configuration is considered. Because all configurations except the T-tail require approximately the same structure, they are assigned the same score of 0. The T-tail is assigned a score of -1 because this configurations requires extra structural reinforcement in the vertical stabilizer in order to support the horizontal stabilizer.

To determine scores for stability, the predicted implications of each airfoil on stability is considered. The conventional tail, when properly designed, is known to give full stability to the aircraft. The T-tail functions in the same way that the conventional tail, and is thus give a score of 0. Although the V-tail lacks the same amount of physical surfaces, yaw coupling in this design gives the aircraft similar stability and is also assigned a score of 0. The actual effect of omitting the rudder control surface form the vertical stabilizer is difficult to predict for an RC aircraft. To account for the predicted small instabilities, the conventional tail without a rudder is assigned a score of -1.

The complexity score for this section refers to the relative complexity of building each design with respect to the conventional tail design. From previous DBF experience, it is known that building a V-tail does not require significantly more effort over a conventional tail, and thus it is given a score of 0. Because the T-tail requires structural reinforcement and additional servos embedded in the vertical stabilizer, it is given a score of -1. The lack of servos and a control surface on the conventional tail without a rudder greatly simplifies construction, thus it is given a score of +1.

After assigning scores to each of these components, the multipliers are applied to each score and totaled. The final results are shown in Table 3.3. The T-tail is least favored, with a score of -3 points. The most favored empennage configuration is the conventional tail without a rudder, with a score of +2 points.

Table 3.3: Empennage trade study results

	(Multiplier)	V-tail	T-tail	Conventional	Conventional w/out Rudder
Servos Required	**2**	**0**	**0**	**0**	**+1**
Weight	**2**	**0**	**-1**	**0**	**0**
Stability	**1**	**0**	**0**	**0**	**-1**
Complexity	**1**	**0**	**-1**	**0**	**+1**
Total		**0**	**-2**	**0**	**+1**

3.2.3 Wing Controls Selection

In order to select a preliminary wing control, a trade study was performed to compare the benefits of certain features. The team considered four different types of designs: wings with 1 aileron, 2 aileron, 1 aileron with flaps and 2 ailerons with flaps. The 2 aileron with flaps was set as the benchmark to compare to and given a score of zero.

To assign scores for the weight of each servo, a 10% increase compared against the HITEC-HS-65 was considered to be a -1 point. The reason being that a servo that is lighter with sufficient torque and speed would be more preferred. Therefore, the 1 aileron, and the 1 aileron with flaps configurations would weigh less than the 2 ailerons and would improve the plane's score.

To score the stability, it was assumed that 2 ailerons with and without flaps were the most stable. Therefore the 1 aileron with and without flaps received a -1 score.

To calculate the complexity, it was assumed that the 1 aileron design was the least complex because it required the least amount of servos as well as the least amount of parts needed. It was decided that the aileron with 2 flaps would be the most complex because there is the most servos and the most parts to create both the flaps and the aileron.

Overall, it is concluded that 1 aileron would be the most beneficial if the turning control for the aircraft is to be attained from the wing. It requires the least servos, which is extremely important for the competition scoring. It also weighs the least and is the least complex. In order to account for the case in which the flight controls are limited to just a rudder and elevator (no ailerons) this option was included as well.

Table 3.4: Wing controls trade study results

	(Multiplier)	1 Aileron	2 Ailerons	1 Aileron w/ Flaps	2 Ailerons w/ Flaps	No Ailerons / No Flaps
Servos Required	**2**	**+1**	**0**	**-1**	**-2**	**+2**
Weight	**2**	**+1**	**0**	**0**	**-1**	**+2**
Stability	**1**	**-1**	**0**	**-1**	**0**	**-2**
Complexity	**1**	**+1**	**0**	**-2**	**-3**	**+3**
Total		**3**	**0**	**-1**	**-3**	**5**

3.2.4 Final Controls Selection

The results of the empennage and wing controls section indicate that an airplane controlled with either an elevator and one aileron or an elevator and rudder would be the best fit for this competition. The goal of this section is to summarize the analysis of these two control configurations, which sought to find the most beneficial configuration. The first prototype, shown in Figure 3.12, was constructed specifically intended to test these configurations. The results in the air proved to be fairly consistent with the predictions in the trade studies, however on the ground, significant advantages were apparent in the rudder and elevator control configuration. The rudder allowed for ground steering, which helped the aircraft to track along the runway on both take-off and landing. Additionally, when a cross wind was present, the rudder enabled far superior directional control on take-off and landing than the single aileron configuration. Due to the superior ground controllability of the rudder and elevator control system, it was chosen as the configuration for the competition.

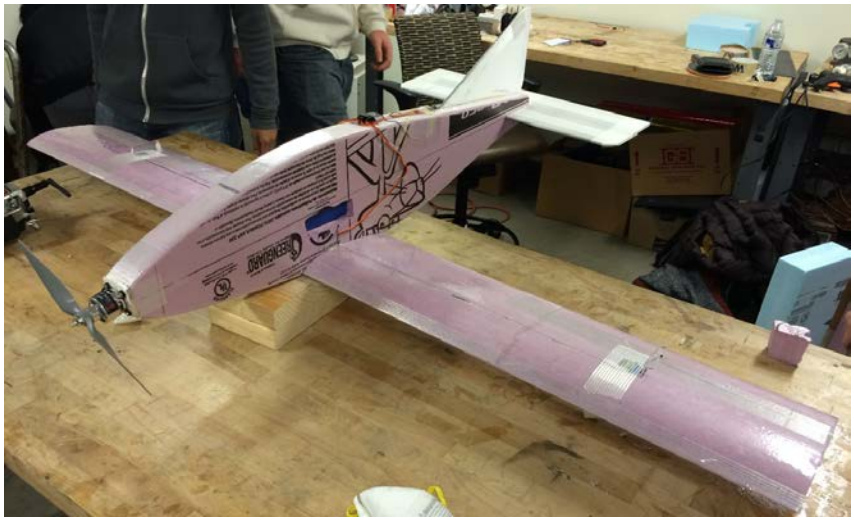

Figure 3.12: Controls prototype

3.2.5 Fuselage Selection

The goal of the fuselage selection was to compare several fuselage shapes and designs, each one meant to maximize aerodynamic efficiency and structural integrity, while minimizing weight and complexity. Each design also must meet the requirement of completely encasing the internal payload and allow space to mount the external payloads.

The method used for defining the shape of the fuselage was to search airfoils which could be scaled to house the internal payload and systems, while maintaining an adequate tail moment which would be defined by the shape of the airfoil. The airfoils chosen as candidates for the fuselage were all symmetrical, so that there would be a minimal moment introduced by the fuselage. The airfoil which

best fit the shape and had the best drag properties of the selected airfoils was the NACA 63(3) – 018, shown below in Figure 3.13.

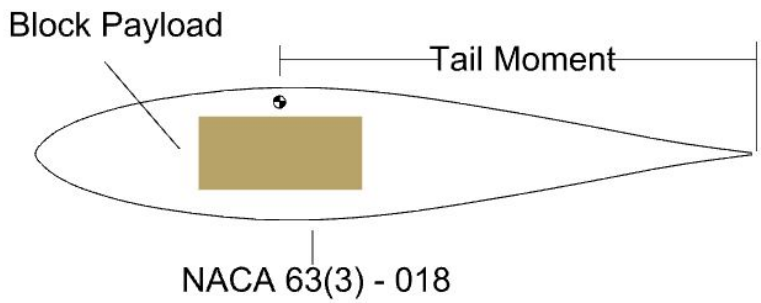

Figure 3.13: Airfoil-shaped fuselage schematic with the payload

Because the power system trade studies selected the single engine tractor configuration for the competition, the conceptual fuselage design assumed the motor to be mounted at the leading edge of the airfoil.

3.2.6 Landing Gear Selection

The goal of the landing gear selection was to find a stable, controllable, and lightweight configuration that provided adequate clearance for the external sensor payloads. Three configurations were considered, as shown in Figures 3.14 through 3.16: tail dragger, quad gear, and tricycle gear.

Figure 3.14: Tail dragger

Figure 3.15: Quad gear

Figure 3.16: Tricycle gear

A trade study was conducted to compare the features of each configuration. The scoring parameters are; weight, stability, and controllability. A score of 0 was assigned to the tail dragger configuration for all parameters.

Table 3.5: Landing gear trade study results

	Weight	Stability	Controllability	Total
Tail Dragger	0	0	0	0
Quad Gear	-2	1	-1	-2
Tricycle Gear	-1	1	-1	-1

For the weight category, the quad gear was given a score of '-2' due to the fact that it required two significant hard mounts and significantly more structure than the tail dragger configuration. It also requires two sets of wheels and landing legs. For the stability category the quad gear was given a score of '+1' because it would provide superior directional stability on the ground, however the tradeoff with this is a reduced degree of controllability resulting in a '-1' for that category. The tricycle gear configuration was given a score of '-1' for the weight category due to the relatively higher structural strength required for the nose wheel than a simple tail skid, as would be used in a tail dragger. However due to having a third wheel on the nose, the directional stability of a tricycle gear configuration is superior to that of a tail dragger, resulting in a '+1' for the stability category. From a controllability standpoint, tricycle gear is inferior to the tail dragger in this case and thus received a '-1' score. The logic behind this decision was that in a tricycle gear configuration, the extra servo and/or linkage required to make the nose wheel steerable outweighs the benefit of having a steerable nose. This means that if a tricycle gear configuration was selected, a steerable nose wheel would not be implemented and ground steering would be limited when compared to the simple steerable tail wheel used in a tail dragger configuration. For these reasons, a tail dragger configuration was selected for the competition.

3.2.7 Conceptual Dropping Mechanism Design

The preliminary goals in the design of the dropping mechanism were to minimize weight, number of servos, time required to affix to the plane and structural complexity/volume while maximizing reliability and optimizing the number of plastic balls carried. Because the sensor drop mission is not a speed mission, rather more of an endurance mission, it was determined that sacrificing the clean, aerodynamic profile of missions one and two in order to improve the aerodynamics of mission three did not make sense. Because of this, no fairings or protruding parts were included in the design of the mechanism. This minimalistic approach was carried out throughout the design of the dropping mechanism. In order to reduce the total number of servos on the plane, it was proposed that a single servo should be used to control the entire mechanism. To even further reduce the number of servos, a goal was set to combine the function of the elevator and the

dropping mechanism into one servo. These goals were determined to be important regardless of the dropping configuration, and thus the only variables that needed to be discussed in the trade study were the number of balls carried and the configuration in which they were to be carried. The first trade study looked at the number of balls carried. The range of 1-10 plastic balls was selected due to the necessity of carrying at least one plastic ball, and the estimated battery life limiting the number of laps to a maximum of about 9 with a 2 lb. battery. The 4-6 plastic ball configuration received a '0' score for each category as baseline.

Table 3.6: Dropping mechanism trade study results

# of Plastic Balls	Structural	Weight (Battery)	Score (for laps only)	Total
1-3	+1	0	-3	-2
4-6	0	0	0	0
7-9	-2	-2	+3	-1

For the structural category, the 1-3 plastic ball configuration received a '+1' vote because it would minimize the structure required to carry the payload. In the weight category, which pertains to the extra battery required to drop every payload in an individual lap, the 1-3 plastic ball configuration received a '0' score. This is because the minimum lap capability of the aircraft must be four laps, regardless of the number of plastic balls carried, in order to complete flight missions one and two. This means that there is no difference in the battery requirement for the 1-3 and 4-6 configurations. In the score category, the 1-3 configuration received a '-3' vote due to the diminished mission 3 score, which is a multiple of the number of balls dropped.

The 7-9 plastic ball configuration received a score of '-2' in the structural category due the extra structure required to carry and drop each ball. The reason a '2' was chosen instead of a '1' is because at the 7-9 plastic ball mark the fuselage length may need to be increased. In the weight category, the 7-9 configuration received a score of '-2' due to the additional battery required in order to sustain flight for any laps after the four lap mark. In the score category the 7-9 configuration received a '+3' score because the additional plastic balls carried would increase the mission 3 score, as described above.

The result of this trade study meant that a plane which carried between 4 and 6 plastic balls should be used for the competition, unless the drawbacks of the 7-9 configuration could be minimized in the design.

The next trade study was conducted to assess the possible layouts of the plastic ball payloads. The three layouts considered were; length wise, span wise, and side by side. Figures 3.17 through 3.19 depict these layouts.

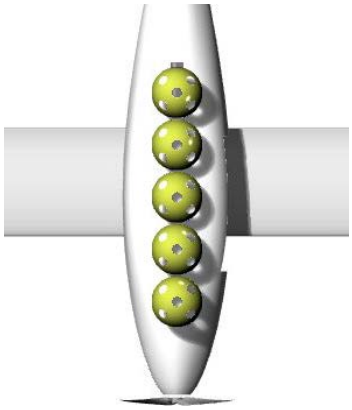

Table 3.17: Lengthwise

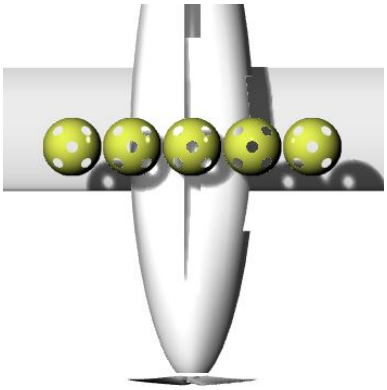

Table 3.18: Span-wise

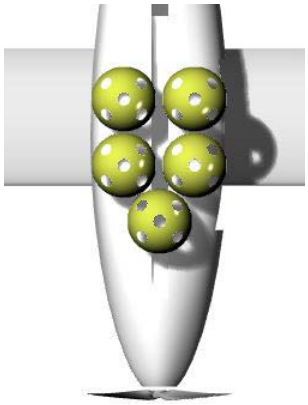

Table 3.19: Side-by-side

The parameters discussed in the trade study were complexity and aerodynamics. The 'length wise' category was given a '0' score for both parameters as a baseline.

Table 3.7: Complexity and aerodynamics trade study results

	Complexity	Aerodynamics	Total
Length Wise	0	0	0
Span Wise	0	-2	-2
Side-by-Side	-1	-1	-2

The span-wise configuration was given a score of 0 for the complexity category because it was not foreseen to increase the structural or mechanical complexity from a length wise configuration. In the aerodynamics category the span-wise configuration was given a '-2' due to the considerably increased cross-sectional area, and disturbed flow when compared to the baseline case. The side-by-side configuration was given a score of '-1' for complexity because the actuation system involved with dropping the balls was expected to increase in complexity if this configuration was used. In the aerodynamics category the side-by-side configuration was given a '-1' because it had a medium cross sectional area and disturbed flow when compared to the other two configurations. The result of these trade studies lead to the conclusion that 4-6 plastic balls should be carried in an inline length-wise configuration.

4. Preliminary Design

4.1 Analysis Methodology

In order to determine important design parameters and make major design decisions, the DBF team at UW utilized multiple computational software programs to perform analysis. The initial wing sizing was hand calculated, while the airfoil was selected by comparing the characteristics of different airfoils in the NACA airfoil database. A CAD model was completed in *SolidWorks* and CFD

analysis was conducted in the *SolidWorks* Flow simulation application. Through CFD, basic aerodynamic characteristics of wing and fuselage are determined separately, and the characteristic for the whole aircraft was estimated by making reasonable assumptions. The estimated lift, drag and drag build up are calculated based on the CFD results. Design decisions made for the fuselage, empennage, energy and propulsion system came from trade studies and MATLAB models.

4.2 Mission Model

In order to obtain sufficient knowledge of what the aircraft is required to perform during the competition, a 3D course model was constructed for the purpose of analyzing each flight segment. The model is displayed in Figure 4.1. Since the only requirement for landing is to successfully land without significant damage to the aircraft, and the parameters for landing don't affect the flight score, the landing segment is not modeled in the 3D course.

During takeoff, the power provided from the propeller needs to be strong enough to successfully take off within the given take off length. With an empty load, the aircraft need less power to take off within the same take off distance than a fully loaded aircraft. Therefore, ensuring that the aircraft can take off within 60 ft. with its maximum load (for the second flight mission) also ensures a successful take off for other missions. To quickly take off with the heavy payload, the airfoil selected needs to have a large coefficient of lift and stall angle, and the wing area needs to be great enough to generate sufficient lift.

During cruise, the aircraft needs to be able to maintain its altitude at a small angle of attack.

The aircraft should have the capability to pull a turn without overloading the wing; thus, structural tests for multiple G's is required to ensure the turning can be successfully performed.

For the sensor dropping mission, the aircraft must have enough stability to give the pilot control over timing the location for dropping the plastic balls.

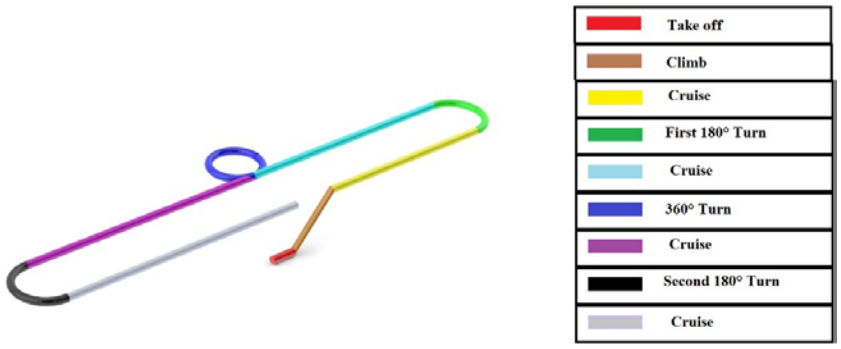

Figure 4.1: 3D course model

The major uncertainty concern is the wind conditions in Marana, Arizona, which will heavily effect the aircraft's performance due its light weight and the externally-mounted plastic balls. Strong headwinds can significantly increase the time to complete a turn, which will also increase the total

flight time. The battery endurance therefore needs to be sufficient to account for this possible change in flight time. To minimize the effect of a strong headwind, it is necessary to avoid exceedingly low wing loading, i.e., the wing area should be minimized while still generating enough lift. Adequate control and a strong enough aircraft structure are also needed to enable the aircraft to turn successfully in strong headwind conditions. Another source of uncertainty comes from the inconsistency of the cells in the battery pack. This requires the team to perform multiple battery tests to be able to predict this variance. According to the AIAA DBF contest website, the payload for mission 2 given in the competition has a tolerance of ±1/8 in in all directions from its nominal dimension. It is the UW team's responsibility to take that uncertainty into consideration and make a large enough payload bay to accommodate the change in dimensions of the payload.

4.3 Design and Sizing Trades

4.3.1 Fuselage Design

The result of the conceptual design phase determined that the fuselage shape should be defined by an airfoil encasing the internal payload, structures, and subsystems. The airfoil chosen to define the fuselage shape was selected based on how well it fit the payload, the tail moment arm it produced, and the drag it produced. The final airfoil selected was the NACA 63(3) – 018 symmetrical airfoil. This preliminary design proposal is shown below in Figure 4.2.

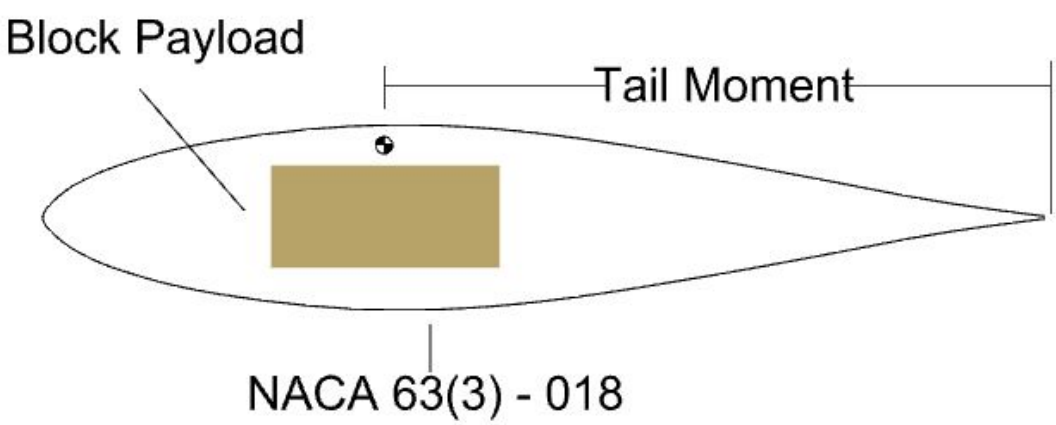

Figure 4.2: Aircraft fuselage based on the NACA 63(3) - 018 symmetric airfoil

Once an airfoil was selected to define the fuselage top and side profile shapes, a cross sectional shape needed to be defined. In order to maximize favorable aerodynamic characteristics such as stability, drag, and cross-wind flying capabilities, the design of the cross-sectional shape sought to minimize corners and sharp edges. The result was a rounded cross-section, varying between

circular shapes for the motor mount and tail and a rounded square-like shape surrounding the payload. Figure 4.3 depicts the cross section.

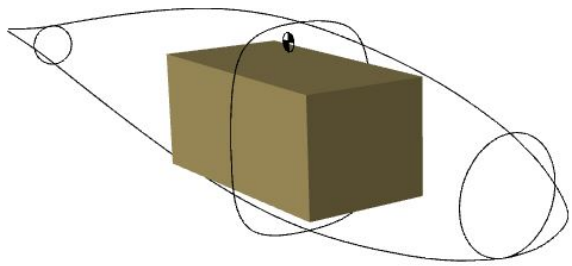

Figure 4.3: Cross-sectional area of the fuselage with block payload

The NACA 63(3) – 018 and the cross-sectional shapes allowed an entire fuselage shape to be defined. Once this was defined in SolidWorks, the fuselage was run through the built-in CFD function. An image of this analysis is shown below in Figure 4.4.

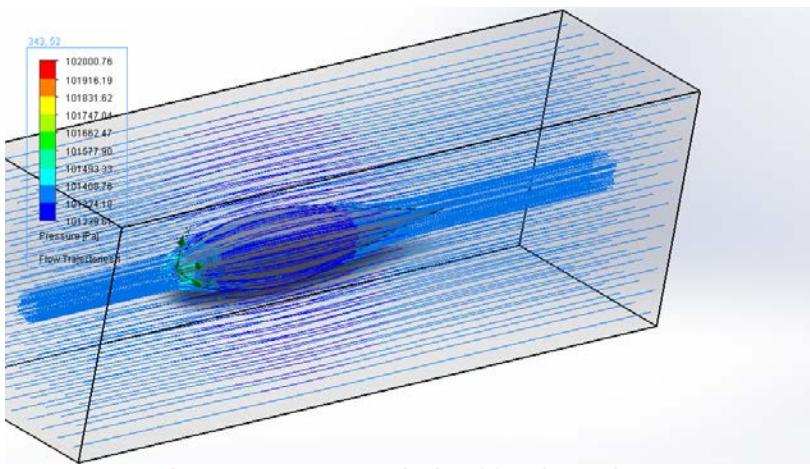

Figure 4.4: CFD analysis of fuselage shape

The CFD analysis verified the predictions made for the fuselage drag values and sideslip performance, and the model analyzed was accepted as the competition fuselage shape.

4.3.2 Tail Sizing

The method used to predict the required vertical and horizontal stabilizer areas employed the use of tail volume coefficients. The formulas which define the tail volume coefficients, V_H and V_V, are shown below.

$$V_H = \frac{L_H S_H}{S_w (MAC)} \tag{4.1}$$

$V_H = horizintal\ tail\ volume\ coefficient$; $L_H = horizontal\ tail\ moment\ arm$;

$S_H = horizontal\ tail\ area$; $S_w = wing\ area$; $MAC = mean\ aerodynamic\ chord$

$$V_V = \frac{L_V S_V}{S_w(Span)} \tag{4.2}$$

$V_V = vertical\ tail\ volume\ coefficient;\ \ L_V = vertical\ tail\ moment\ arm;\ \ \ Span = wing\ span$

Fundamentals of Aerodynamics, by Anderson, J.D. [2] has multiple chapters describing acceptable tail volume coefficients for various aircraft types, and DBF at the University of Washington had a repository of numbers used from previous years. Using these two resources the tail volume coefficients to be used were determined. The following values were selected:

$$V_H = 0.5, \qquad V_V = 0.08$$

The moment arm length of 24 inches for the horizontal and vertical stabilizer was determined by the NACA 63(3) – 018 airfoil used to define the shape of the fuselage, as shown in Figure 4.2. The required area for the vertical and horizontal stabilizers was then calculated as a function of the wing area and wingspan, and are shown below.

$$S_H = 83.33\ in^2, \quad S_V = 56.66\ in^2$$

4.3.3 Airfoil Selection

The 3 candidates for the UW's airfoil selection were picked from the NACA 6-series. The main reason being that the characteristics of NACA airfoils are well-documented, therefore creating less obstacles for the analysis process. The 6-series was designed for maximizing laminar flow, which serves the missions' needs. The maximum coefficient of lift versus coefficient of drag were compared among the NACA 63(2)-615, NACA 63-215 and NACA 63-415 [3]. These three airfoil were selected because they demonstrated good lift performance among the NACA 6 series. The Reynolds number range was selected to be around 300,000 with an approximate maximum cruise speed of 30 m/s. Figures 4.5 through 4.8 depict C_l/C_d, C_l vs.α, C_m vs. α and C_d vs. α curves, respectively. Note that the green curve represents NACA 63(2)-615, the yellow curve represents NACA 63-415 and the red curve represents NACA 63-215.

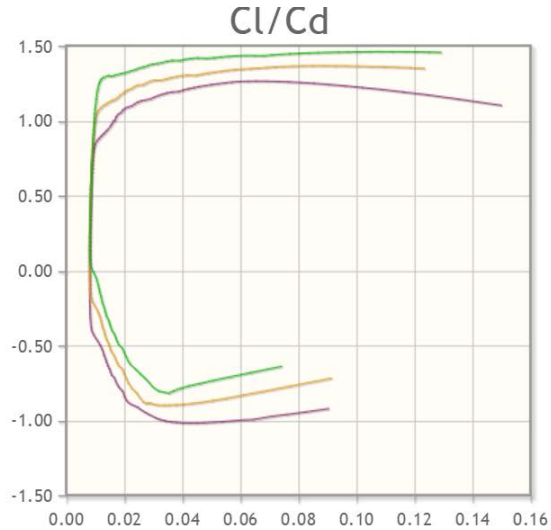

Figure 4.5: C_l vs. C_d

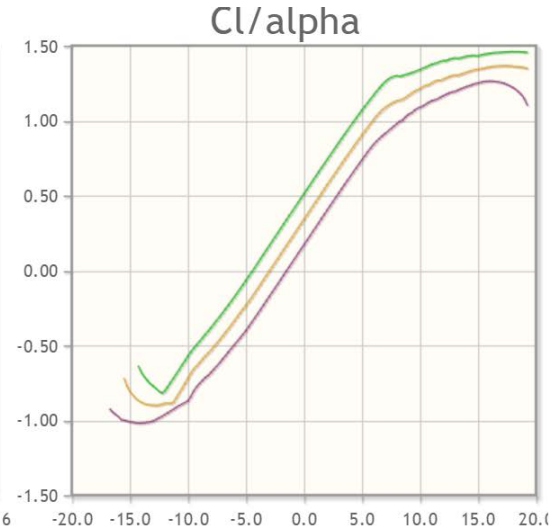

Figure 4.6: C_l vs.α

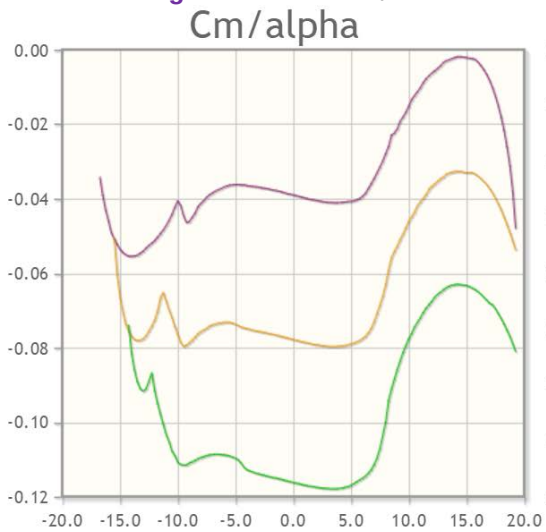

Figure 4.7: C_m vs. α

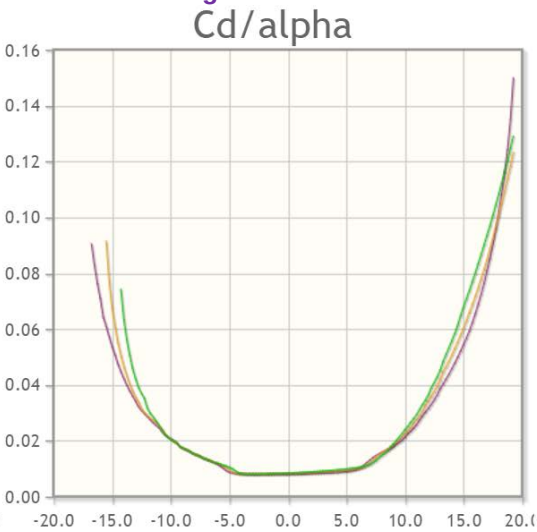

Figure 4.8: C_d vs. α

As shown in the graphs, the green curve stands out for C_l/C_d, which means NACA 63(2)-615 can generate higher lift while producing lower drag. Pitching moment of three airfoils are all negative, while for NACA 63(2)-615, the magnitude was bigger, which indicates higher stability. The data of maximum C_l /C_d is tabulated in Table 4.1 below.

Table 4.1: Maximum C_l /C_d comparison

	NACA 63(2)-615	NACA 63-215	NACA 63-415
MAX C_l / C_d	81.7	65.5	75.6
α @ which it occurred	7.5°	7°	7.25°

From Figure 4.9, even if the aircraft does not reach angle of attack as high as 7°, the coefficient of lift of NACA 63(2)-615 is always the largest. Combining all the factors discussed above, airfoil NACA 63(2)-615 was selected for the wing. The airfoil chosen for the fuselage was discussed in the Section 4.3.1; the airfoil chosen for the horizontal tail is NACA 0012, which is a laminar flow symmetrical airfoil that was found to have low drag. Since the vertical tail is not designed to provide lift, the shape was selected to be a thin flat plate, which has the least frontal area.

CFD analysis was also done for a wing segment in order to verify the airfoil data from the NACA airfoil database. Figure 4.9 was captured during the flow simulation over the wing segment.

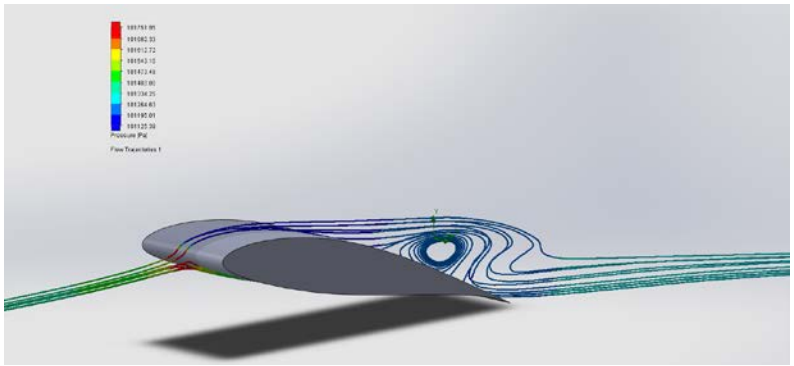

Figure 4.9: Flow simulation over the wing segment

Figure 4.10 depicts the lift-to-drag ratio of the wing segment versus angle of attack. It indicates that the aircraft should not exceed 12° angle of attack during the competition to avoid stalling.

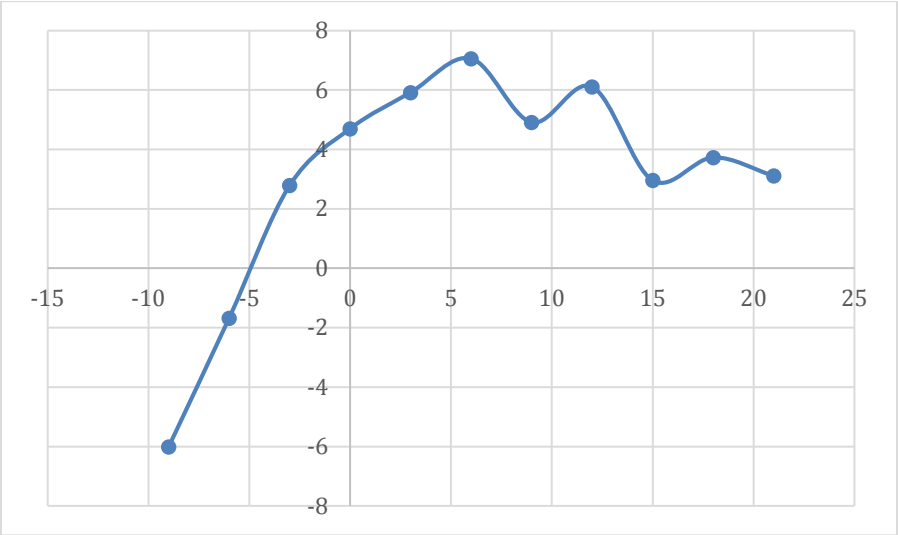

Figure 4.10: L/D trend over angle of attack

4.3.5 Propulsion System

The main goals of the propulsion system selection were to maximize thrust, minimize weight, and ensure adequate endurance for the sensor drop mission. The analysis involved in the selection of this year's system differed from previous years due to the fact that there is no required current limit. This shifted the focus from maximizing thrust for a given current to optimizing the parameters of the system, such as weight and thrust. In order to accurately estimate performance characteristics of different propulsion configurations (motor type, battery type), a performance model in MATLAB was created. This model analyzed the thrust, current and RPM of different motor, propeller and voltage combinations. In order to take into account the weight of the battery, the voltage parameter was varied by the voltage of one NiMH cell, and the weight of a single cell was multiplied by the step number. A 3% packaging weight was applied to each battery pack. The performance model was comprised of equations describing a standard steady state DC electric motor. Equations (4.3), (4.4) and (4.5) describe the motor model.

$$RPM = K_V(V_B - V_P) \tag{4.3}$$

$RPM = rotations\ per\ minute\ of\ motor\ w/\ propeller$ $\quad K_V = voltage\ constant\ for\ a\ DC\ motor$

$V_B = voltage\ to\ battery\ via\ throttle\ control$ $\quad V_P = voltage\ drop\ due\ to\ propellor\ load$

$$V_P = IR \tag{4.4}$$

$I = current\ draw\ of\ the\ motor,\ as\ a\ function\ of\ RPM\ and\ Propeller\ coefficient\ C_P$

$R = constant\ resistance\ of\ the\ system,\ estimated\ from\ manufacturer$

The final function for the RPM of the motor becomes:

$$RPM = K_V(V - I(RPM, C_P)R) \tag{4.5}$$

As shown in equation (4.5), RPM is a function of itself. Because of this the model cannot be directly solved and an iterative "for loop" was implemented in MATLAB. The thrust of a propeller is quite easily calculated if the RPM is known, due to well documented test data for APC propellers. The data available on APC's website was analyzed to obtain a range of propeller thrust coefficient values which relate the thrust to the RPM. Instead of mathematically deriving these values we chose to rely on the test data presented on the website for each specific propeller used. This allowed us relate thrust to voltage, current, motor K_v, weight and propeller type. Weight of the propulsion system was defined as ('1.03' accounts for the 3% packaging weight):

$$W_P = W_m + 1.03(N_C W_C) \tag{4.6}$$

$W_m = motor\ weight$ $\quad N_C = number\ of\ battery\ cells$ $\quad W_C = weight\ of\ battery\ cell$

With a propulsion model completed, the next step was to implement different motor, propeller, and battery pairs until a combination was found that allowed for maximum thrust and minimum weight. A minimum acceptable thrust value was set to the required thrust to take off in 60 feet with an

estimated aircraft weight of 8lbs. Due to the fact that 8 lb. incorporates quite a large safety factor, it was assumed to be an adequate minimum, especially because the optimization model continually picked much higher thrust values than this minimum. Because the scoring analysis revealed weight to be a more significant factor in the score than speed, this optimization model gave weight an importance multiplier of 1.3 relative to thrust. Once an optimized thrust value was found, different motors, propellers, and battery voltage combinations were selected to match with values from commercial products. The result of testing led to the selection of an AXI-2820/12 990 kV Gold Line electric motor, APC 12x6 E propeller, 14 ELITE 1500 mAh battery cells wired in series.

4.3.6 Wing Geometry

In order ensure adequate lift is produced from the wing, the following function was used to relate the lifting force, air density, velocity, coefficient of lift and wing area.

$$Lift\ Force = \left(\frac{1}{2}\right)\rho v^2 \cdot C_L \cdot S_w \tag{4.7}$$

$\rho = air\ density\ (in\ Arizona\ during\ April)$ $\quad$ $v = cruise\ velocity$

$C_L = coefficient\ of\ lift\ (at\ cruise\ alpha)$ $\quad$ $S_W = Wing\ Area$

The maximum estimated weight of the final aircraft, 8lbs or 35.6 N, was set equal to the lift force in equation (4.7). The CL of the NACA 63(2) at a cruising alpha of 2° was determined to be .65, and the estimated cruise velocity was 20 m/s. During April, the average air density in Marana, AZ is 1.2 kg/m^3 according to the National Oceanic and Atmospheric Association. Based on these values, the minimum required wing area to carry 8lbs at cruising speed and given alpha is:

$$.22\ m^2\ or\ 356\ in^2$$

It is important to note that this value pertains to the minimum necessary wing area at cruising speed, and does not take into account the lower landing and takeoff speeds. In previous years, the DBF team has used a multiplier of 1.4 to derive the required wing area for takeoff and landing speeds from the minimum cruise area. When this multiplier is applied, the required wing area becomes:

$$Required\ Wing\ Area = 498.4\ in^2$$

The wing tip was chosen to be dome shaped based on the CFD result of multiple types of wing tips, as the dome shaped wing tip provides the largest the lift to drag ratio. Table 4.2 shows the comparison between the dome shaped wing tip with other types of wing tip at a 2 degree angle of attack, which demonstrate the cruising condition. Figure 4.11 captured the CFD analysis in progress for the dome shaped wing tip via the SolidWorks Flow Simulation.

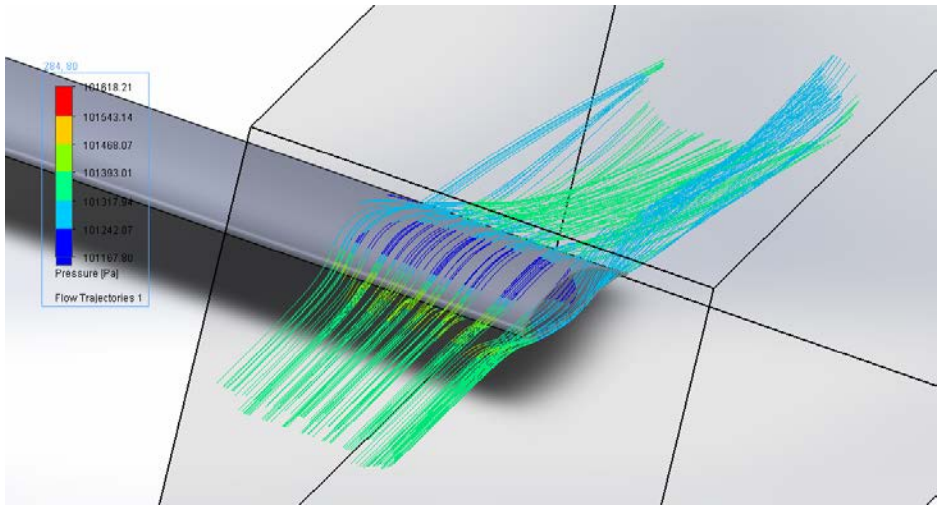

Figure 4.11: Flow simulation for dome shaped wing tip

Table 4.2: Lift-to-drag comparison for various wing tip features

Feature	Lift (N)	Drag (N)	L/D
No Feature	0.034151869	0.009276911	3.68
Dome	0.031849053	0.006404941	4.97
Swept Up	0.060873239	0.01694669	3.59
Hoerner	0.06004258	0.012972239	4.63

CFD analysis was also done for a wing segment in order to verify the airfoil data from the NACA airfoil database. Figure 4.12 depicts the lift to drag ratio of the wing segment versus angle of attack. It indicates that the aircraft should not fly at a higher angle of attack of 12 degrees in the competition.

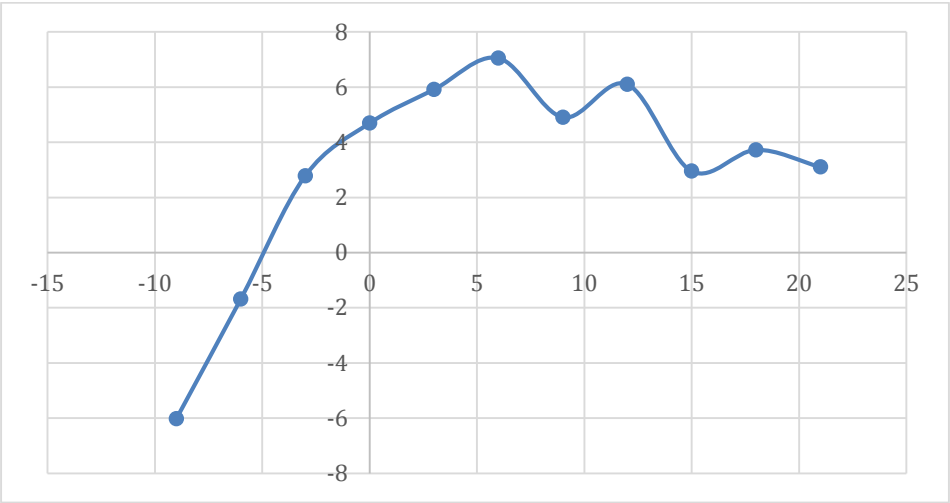

Figure 4.12: L/D trend over angle of attack

4.4 Lift, Drag and Stability Characteristics

Due to the limitation of CFD software at hand, the team was not able to perform CFD analysis for the entire aircraft model. Therefore, the lift and drag were analyzed separately for individual parts of the aircraft.

Using SolidWorks Flow Simulation, the lift and drag characteristics of the wing and fuselage are analyzed, respectively. Since the polyhedral wing is deflected at the center, the torque created by the deflected lift component towards the fuselage is also evaluated to ensure the connection between the flat panel and the deflected panel has enough strength to handle the torque. The torque towards the fuselage is 6.54487 [N*m] at cruise condition. The CFD analysis of the fuselage can be seen in Figure 4.13.

The lift and drag characteristics of the wing on one side and fuselage are tabulated in Table 4.3. The lift and drag value of the wing were evaluated at two degree angle of attack, while the fuselage was at zero angle of attack, as it was the relative position of the wing and fuselage during cruising. The flow speed was set to 25 m/s.

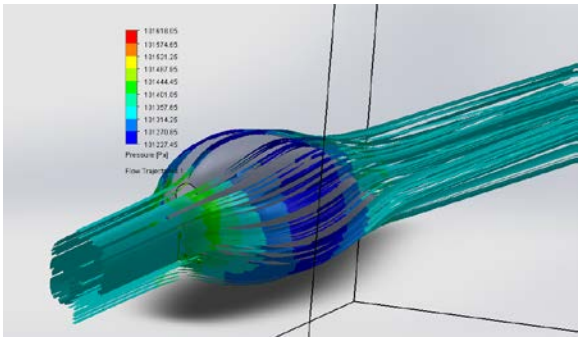

Figure 4.13: CFD analysis of the fuselage

Table 4.3: Lift and drag characteristics of the wing and fuselage

	Wing	Fuselage
Lift (N)	16.20125	0.02401625
Drag (N)	1.906613	0.8805356
L/D	8.497398	0.02727459

Estimated Lift

Since the only part on the aircraft that generate significantly amount of lift is the wing, the total estimated drag was simply two times the lift generated by the wing on one side. Based on the result of the CFD analysis, the total estimated lift is determined to be 32.43 N, i.e., 7.3 lb., which is approximately the maximum weight of the aircraft. Higher lift can be achieved by pulling higher angle of attack and increasing the cruising speed.

Estimated Drag

Parasitic drag for the dropping mechanism, the horizontal stabilizer, the vertical stabilizer and the landing gear is estimated by the frontal area estimation method (Figure 4.14). The coefficient of friction for all parts is estimated to be 0.0035 as all the airframe is laminated by Monokote, the frontal area of the landing gear is so small that the variation in coefficient of friction can be neglected, and the boundary layer around the plastic balls is predicted to be very thick so that the variation in coefficient of friction of the plastic balls is not significant.

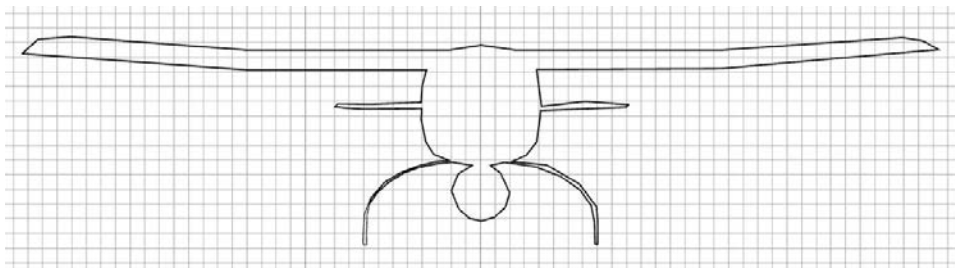

Figure 4.14: Frontal area estimation from *Rhinoceros*

The induced drag for the horizontal stabilizer is calculated by Equation 4.8:

$$D_i = \frac{L^2}{\frac{1}{2}\rho v^2 S\pi e AR} \tag{4.8}$$

Where L, S and AR is the lift, surface area and aspect ratio of the part being evaluated, ρ is the flow density, v is the flow velocity, and e is the wing span efficiency value.

The induced drag for other parts are neglected, since the other parts don't generate lift. The total drag from the wing and the fuselage were obtained from the CFD analysis.

Through careful calculation of the drag contributed by each part of the aircraft, the total drag was estimated to be 1.12 lb., which is close to the thrust needed at a 25 m/s cruising speed.

The drag build up chart is shown in Figure 4.15 below.

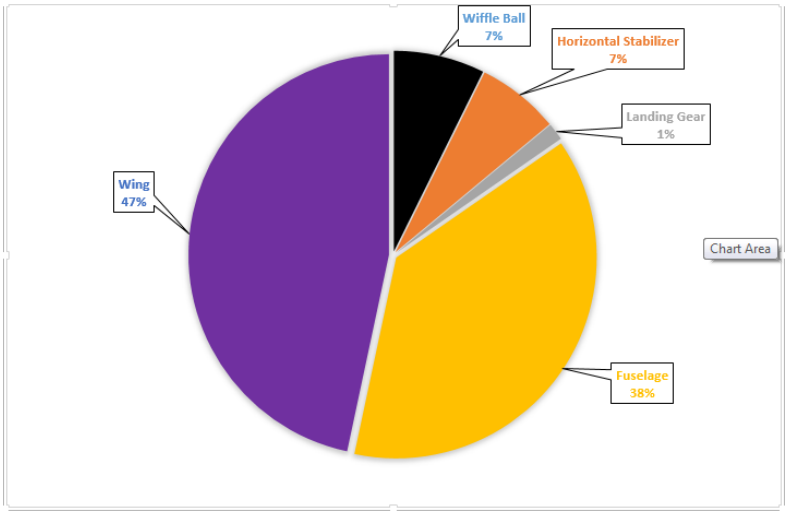

Figure 4.15: Drag distribution at cruising conditions

Stability and Control

Static stability was achieved by designing the vertical and horizontal stabilizers to be adequately sized, based on the analysis covered in the tail sizing section. Dynamic stability, which is an aircraft's ability to damp out momentary disturbances, depends on the mass distribution throughout the aircraft. In addition to ensuring that the aircraft balances at the designated CG, it was important to make every attempt to localize this mass around the CG as much as possible. This is because when in flight, the aircraft will rotate around the CG, and any high mass concentration far from this point will enter into harmonic motion in the event of a disturbance. The closer the mass concentrations are to the CG, the faster the oscillations will be damped out by the aircraft.

However, In order to maintain a level of maneuverability sufficient for the competition course, maximum stability was not the goal. If the aircraft were too stable, it would not respond effectively to control input and thus maneuverability would suffer. This was considered in the sizing of the tails, and was accounted for by only exceeding the minimum required vertical and horizontal tail areas by 10%.

4.5 Predicted Aircraft Mission Performance

Table 4.4 displays the predicted aircraft performance parameters. All the calculation are based on real measurement, airfoil database and CFD analysis.

Table 4.4: Performance parameters for missions 1 through 3

Performance Parameter	Mission 1	Mission 2	Mission 3
Flight Weight	2.6 lbs.	7.6 lbs.	3.34 lbs.
$C_{l,max}$	1.3	1.3	1.3

Motor Efficiency	**0.7**	**0.6**	**0.8**
$C_{D,0}$	**0.023**	**0.023**	**0.023**
Min Takeoff Distance	**8 ft.**	**25 ft.**	**10 ft.**
L/D max	**15.3**	**15.3**	**15.3**
Max Speed (m/s)	**30 m/s**	**22 m/s**	**15 m/s**
Number of Laps	**8**	**3**	**5**
Cruise Speed (m/s)	**25 m/s**	**20 m/s**	**15 m/s**
Flight Time	**4 min**	**2.04 min**	**5 min**
Predicted Score	**2**	**3.5**	**3.75**
RAC	**7.8**		
MAX Empty Weight	**2.6 lbs.**		

As shown, the preliminary design aircraft is highly competitive in this competition, with a RAC of 7.8 and maximum speed of 30 m/s.

5. Detail Design

5.1 Dimensional Parameters

All major dimensions of aircraft are documented in Tables 5.1 and 5.2. These parameters result from extensive studies summarized in the Preliminary Design section. Note that the height of the aircraft also includes the additional height of the landing gear. The dropping mechanism has a 1.13'' height extended out of the fuselage. The dimensions of the aircraft shape determines the structural design and subsystem integration that are discussed later in this section.

Table 5.1: Aircraft dimensions

Aircraft		Fuselage		Dropping Mechanism	
Length	46.57''	**Length**	39.53''	**Length**	19.56''
Width	62.34''	**Width**	8.05''	**Width**	1.00''
Height	18.34	**Height**	8.05''	**Height**	4.19''

Table 5.2: Aerodynamic surface dimensional parameters

Main Wing		Vertical Stabilizer		Horizontal Stabilizer	
Airfoil	NACA 63(2)-615	**Airfoil**	Flat	**Airfoil**	NACA 0012
Span	62.34''	**Span**	6.74''	**Span**	16''
Chord	8''	**Chord**	9''	**Chord**	5.75''
Area	498.72 in^2	**Area**	60.66 in^2	**Area**	92 in^2
Aspect Ratio	7.8	**Aspect Ratio**	0.749	**Aspect Ratio**	2.78
Tip Dihedral	5°				

5.2 Structure Characteristics and Capabilities

The main airframe of the aircraft is made of foam, however, structural reinforcement was implemented in required locations in order to enable the aircraft to bear the expected load during flight.

5.2.1 Motor Mount Piece

Stress analysis of the motor mount piece was done in *FEMAP*. The deformation of the circular motor mount piece is shown in Figure 5.1. Note that the deformation scale is highly exaggerated in the program for visualization.

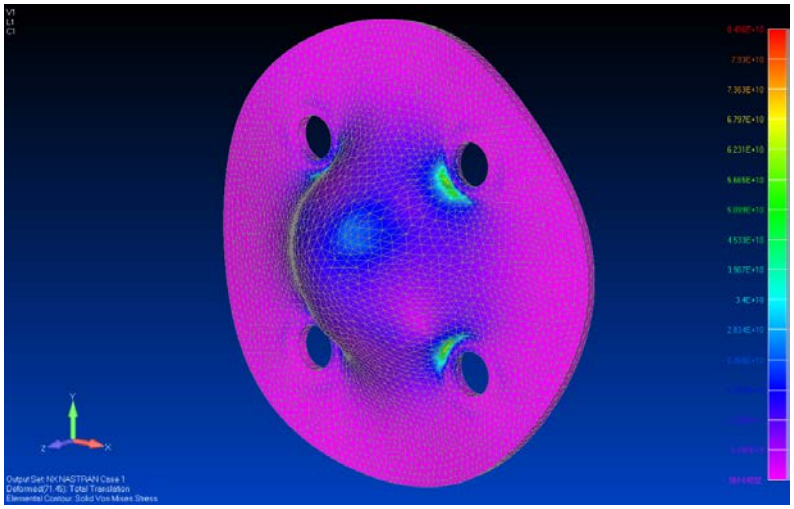

Figure 5.1: Deformation of motor mount piece under the stress from the motor

The material of the motor mount piece is chosen to be plywood. From this stress analysis, the thickness of the piece is determined to be 1/8" in order to be able to bear the stress from the motor.

5.2.2 Wing Spar Structure

The wing spar is composed of three separate carbon fiber tubes. One pultruded carbon fiber tube goes inside the cut out hole in the fuselage, and two roll-wrapped carbon fiber tubes go inside the wing on each side. The pultruded carbon fiber tube has a smaller radius than the roll wrapped carbon fiber tube, so that they can have a 4 inch overlap on each side to ensure sufficient wing spar strength, as shown in Figure 5.2.

Figure 5.2: Wing Spar Composition

The material of tube on the right is also carbon fiber, although it was made transparent for better visualization.

5.2.3 Landing Gear Structure

The landing gear fairing utilizes the same airfoil shape as the fuselage to minimize the contributed drag. The installation of the landing gear is demonstrated in Figure 5.3.

Figure 5.3: Landing gear installation

The wheel is mounted to the landing gear axle. The axle is mounted to the landing gear strut, and also glued to the fairing.

5.2.4 Dropping Mechanism Design

The goal of the dropping mechanism design was to create a light and reliable mechanism which used a minimal amount of servos. The first task at hand was to design a system to hold each plastic ball to the dropping mechanism. In order to do this, the holes present in the balls was taken advantage of and two plywood arms were designed to be inserted into the opening and rotated to hold the ball in place. This is depicted in Figure 5.4.

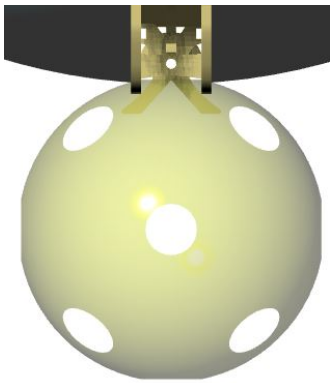

Figure 5.4: Miniature arms holding aplastic ball in place

Once the holding and releasing mechanism had been designed, a mechanism which would allow a single servo to release each individual plastic ball needed to be designed. The trade study

conducted for the payload configuration determined that the plastic balls should be mounted length-wise down the fuselage. This resulted in the decision to implement a system of pins which would keep the holding arms in place until removed from a set of notches cut into the arms. The pins were designed to be of different lengths so that each ball would drop individually. A main strut connected each pin so that they could all be controlled by the elevator servo through a set of notches at the end of this strut. This is depicted in Figure 5.5.

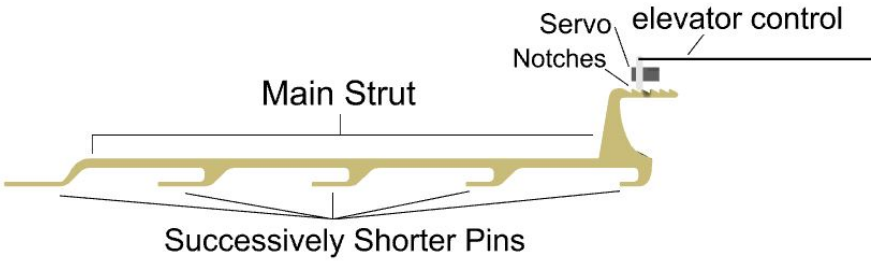

Figure 5.5: Strut, pins, and arm control

The shortest pin was placed toward the rear of the aircraft so that the plastic balls would fall from back to front. This eliminated the possibility of a ball interfering with other mounted balls as it dropped. The strut was designed to move only when the elevator exceeded a specific deflection angle, outside of the deflection range used for normal flight in order to maintain controllability. The holding arm and strut-pin system were held in place by a frame which doubled as a structural backbone for the aircraft and for the dropping mechanism structure. The final mechanism is pictured in Figure 6.6.

Figure 6.6: Dropping mechanism loaded with plastic balls

5.3 Subsystem Design

5.3.1 Battery Selection

In order to narrow down the selection of batteries, a trade study was performed to compare the benefits of different battery types and brands. The overall results of the trade study can be seen in

Table 5.3. The team initially chose Nickel Metal-Hydride (NiMH), as they are superior to Nickel Cadmium (NiCad) in terms of capacity, weight and reliability. NiMH have higher capacities with better energy densities and suffer less from memory discharge. The team considered four types of NiMH batteries: Elite 1500 ⅔ A, Elite 2000AA, Tenergy 2000AA, and the Elite 5000 SC. The Elite 1500A battery was chosen as a basis for comparison since it was the battery utilized in the 1st and 2nd place winners of DBF 2013 and was previously used by UW in DBF 2014. To rate the capacity of each battery, a 20% increase resulted in an additional point (+1). Capacity is weighted at a factor of 1.3 because additional capacity allows the plane to fly for longer periods of time. Reliability is weighted at a factor of 1.5, because poor battery reliability can result in mission failure. Because no published reliability data could be found, all batteries received a score of 0. To assign scores to the weight of each battery, a 10% increase resulted in a score of -1. Weight was set at a factor of 1.3, since heavier batteries will result in a less efficient plane. A 10% increase in volume resulted in the subtraction of a point (-1) for the size category. Size was weighted at a factor of 0.8 since the battery will be stored internally to the system, it has a less significant effect on mission performance. To score the batteries by price, a 10% increase in price resulted in a subtraction of a point (-1). After assigning points, a total score was calculated for each battery. The final results are displayed in Table 5.X. The Elite 5000SC was least favored because it was too costly, too large and too expensive. The most favored, other than the basis, was the Tenergy 2000AA (which had more capacity and the same weight as the Elite 1500 ⅔ A).

Table 5.3: Battery selection trade study results

	(Multiplier)	Elite 1500 ⅔ A	Elite 2000AA	Tenergy 2000 AA	Elite 5000 SC
Capacity	**1.3**	**0**	**+1.5**	**+1.5**	**+5**
Reliability	**1.5**	**0**	**0**	**0**	**0**
Weight	**1.3**	**0**	**-1**	**0**	**-3**
Size	**0.8**	**0**	**-2**	**-2**	**-3**
Price	**1.0**	**0**	**-1**	**-1**	**-3**
Total		**0**	**-1.95**	**-0.65**	**-2.8**

5.3.2 Servo Selection

In order to select a servo, a trade study was performed to compare the benefits of certain features. The team considered four different popular servos: HXT900, DSM-44, HD-1581-HB, and HD-1440A. The HXT900 was set as the benchmark for comparison and was given a score of zero for all features. Some of the most important factors that went into the servo selection were weight, hinge moment provided, and price.

To assign scores for the weight of each servo, a 10% increase from the HXT900 was considered to be a -1 point. A 10% increase in hinge moment was given a +1 point for torque. The DSM-44 and HD-1581_HB both received a score of 0 as their hinge moments were not significantly higher or lower (+/- 10%) than the HXT 900. Since the DSM-44, HD-1581-HB, and HD-1440A all had similar dimensions when compared to the HXT900, they were all given a score of 0 for size. To calculate the scores for the pricing of each servo, a -1 point was given for prices that were 10% more expensive than HXT900.

After assigning these scores to each feature, a total score was calculated for each servo. The final results are displayed in Table 5.4. The DSM-44 is the least favored, as it proved to be too expensive and too heavy while providing the same hinge moment. The most favored servo is the HD-1440A as it is lightweight, but can also provide the sufficient hinge moment during flight.

Table 5.4: Servo selection trade study results

	HXT900	DSM-44	HD-1581-HB	HD-1440A
Size	0	0	0	0
Torque	0	0	0	+1
Price	0	-1	-1	-2
Weight	0	-1	0	+1
Total	0	-2	-1	0

5.4 Weight and Balance

A weight and balance study, the results of which are shown in Table 5.5, was conducted in order to identify each component's contribution to the center of gravity. The data was selected to be at the designed center of gravity, which is approximately at the quarter chord point of the wing. The transverse direction (direction along the wing) is assumed to be perfectly symmetric. The weight and balance table is shown below, which includes each weight component of the aircraft itself, and the two kinds of payloads for the missions of the competition.

Table 5.5: Weight and balance table

Weight Component	CM location (m)	Weight (N)	Torque (N*m)
Fuselage Foam	-0.0875	2.22	-0.19425
Wing Foam	-0.025	1.5	-0.0375
Motor	0.3625	1.1	0.39875

Propeller	0.365	0.075	0.027375
Speed Controller	0.28	0.1	0.028
Rudder	-0.45	0.1	-0.045
Elevator Servo	-0.1	0.1	-0.01
Dropping Mechanism	-0.035	1.2	-0.042
Landing Gear	0.025	0.25	0.00625
Horizontal Tail	-0.6	0.35	-0.21
Vertical Tail	-0.6	0.25	-0.15
Battery	0.1	3.8	0.38
Wing Spar	0	1	0
Motor Mount	0.35	0.075	0.02625
Total Empty		12.12	0.177875
Plastic Balls	-0.025	3.3	-0.0825
Total with Plastic Balls		15.42	0.095375
Wooded Block	0	22.25	0
Total with Wooden Block		34.37	0.177875

As shown, the total torque generated by all the components reduce to a small number compared to the weight of the entire aircraft, which ensures the longitudinal static stability. The overall torque is positive, indicating the aircraft tends to pitch down, which is favorable in terms of obtaining control of the aircraft. Note that the center of gravity of the wooden block payload coincides with the designed center of gravity of the plane, so loading the wooden block should not change the position of center of gravity at all. The center of gravity of the plastic balls is only 1 inch offset from the designed center of gravity. The design limit of the variation of the center of gravity is determined to be 1 inch by flight test, and since the weight of the plastic balls is significantly smaller than all the other weight components combined, the change of center of gravity due to the installation of the plastics balls will not exceed the design limit.

5.5 Performance Parameters

5.5.1 Expected Flight Performance

After the detailed design process, a more realistic estimate of flight performance can be made in order to be compared with the one made at the preliminary design stage. With the detailed structures design, a relatively accurate RAC can be evaluated. According to the scoring formula demonstrated in Section 3.1.1, Eq. 3.4, Rated Aircraft Cost is the product of empty weight and number of servos. The empty weight of the design model is 2.6 lb., and the number of servos of the design model is 3. Therefore, the RAC of the design model is calculated to be 7.8.

The flight performance parameters are obtained in smaller scale flight test and documented in Table 5.6 below.

Table 5.6: Expected flight performance

	Mission 1	Mission 2	Mission 3
Cruise Speed (m/s)	25 m/s	20 m/s	15 m/s
Stall Speed (m/s)	7 m/s	10 m/s	8 m/s
Wing Loading ($\frac{N}{m^2}$)	35.82	104.78	46.06
Rate of Climb (m/s)	5 m/s	2 m/s	3 m/s

5.5.2 Expected Mission Performance

Based on the flight performance determined above, the aircraft model's performance during the missions are estimated as shown in Table 5.7.

Table 5.7: Expected mission performance

	Mission 1	Mission 2	Mission 3
Take-off Weight (lb.)	2.6	7.6	3.34
Number of Laps	8	3	5
Time of Flight (min)	4	2	5
Mission Score	2	3.5	3.75
Empty Weight	2.6		
RAC	7.8		
Total Flight Score	9.25		

5.6 Drawing Packages

A 3D model was constructed in SolidWorks during the design process. The following drawing packages, which were extracted from SolidWorks, include a 3 view drawing of the entire aircraft model, a detailed drawing for the dropping mechanism, a structural alignment drawing, a system layout drawing, and a drawing demonstrating the location accommodating the payloads. The drawings are oriented in order to show as much of the aircraft, and as many of its components, as possible.

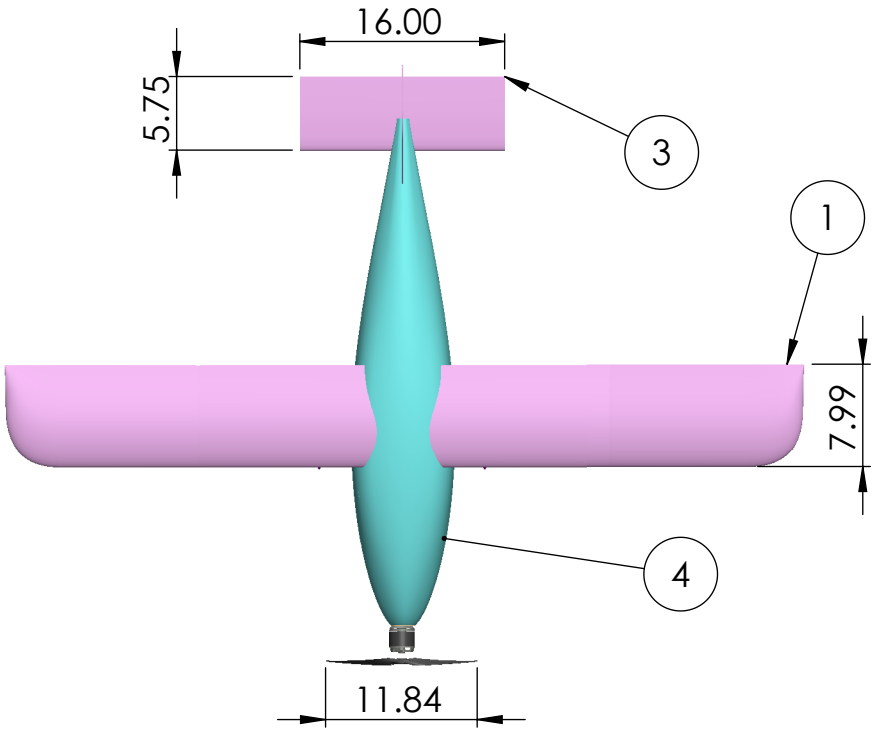

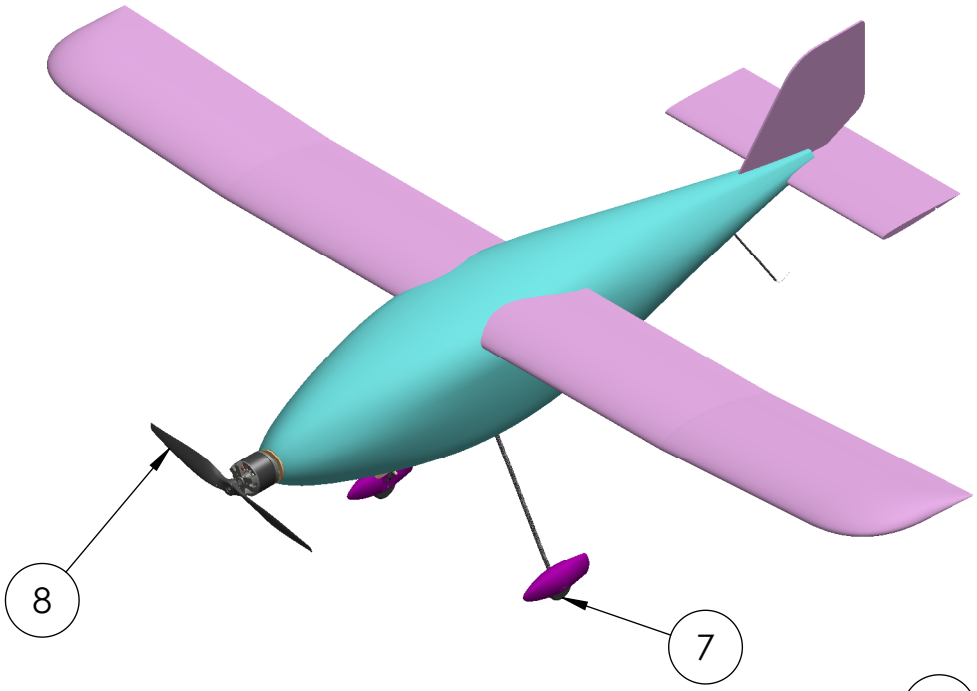

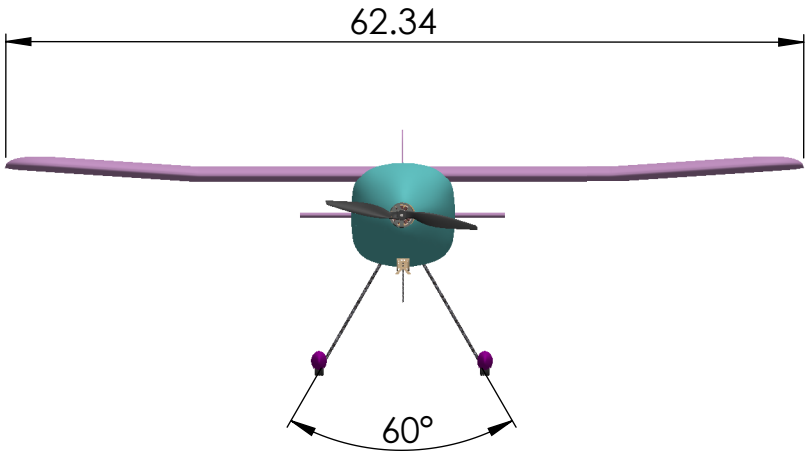

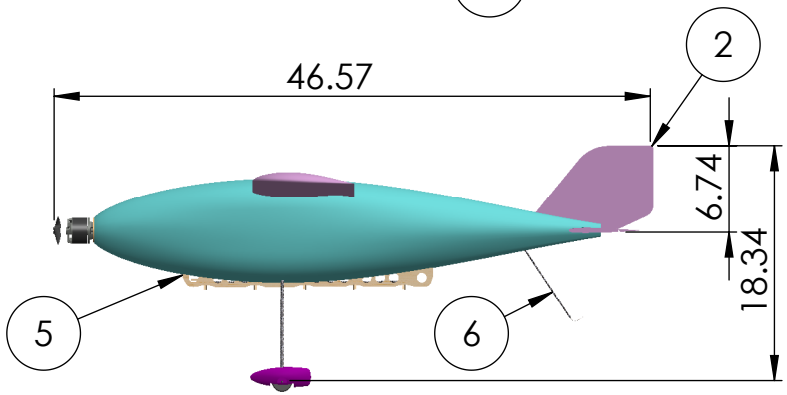

University of Washington

PRIMARY COMPONENTS	
1	WING ASSEMBLY
2	VERTICAL STABILIZER
3	HORIZONTAL STABILIZER
4	FUSELAGE
5	DROPPING MECHANISM
6	TAIL SKID
7	LANDING GEAR
8	PROPELLER

NOTE:
DIMENSIONS ARE IN INCHES
TOLERANCES:
ONE PLACE DECIMAL: ±.100
TWO PLACE DECIMAL: ±.030
THREE PLACE DECIMAL: ±.005

CESSNA - RAYTHON - DESIGN BUILD AND FLY 2014-2015

SIZE **A**

Title: 3 VIEWS - AIRCRAFT

SCALE: 1:15 3 VIEWS - SCALE 1:12 ISOTROPIC VIEW

SHEET 1 OF 1

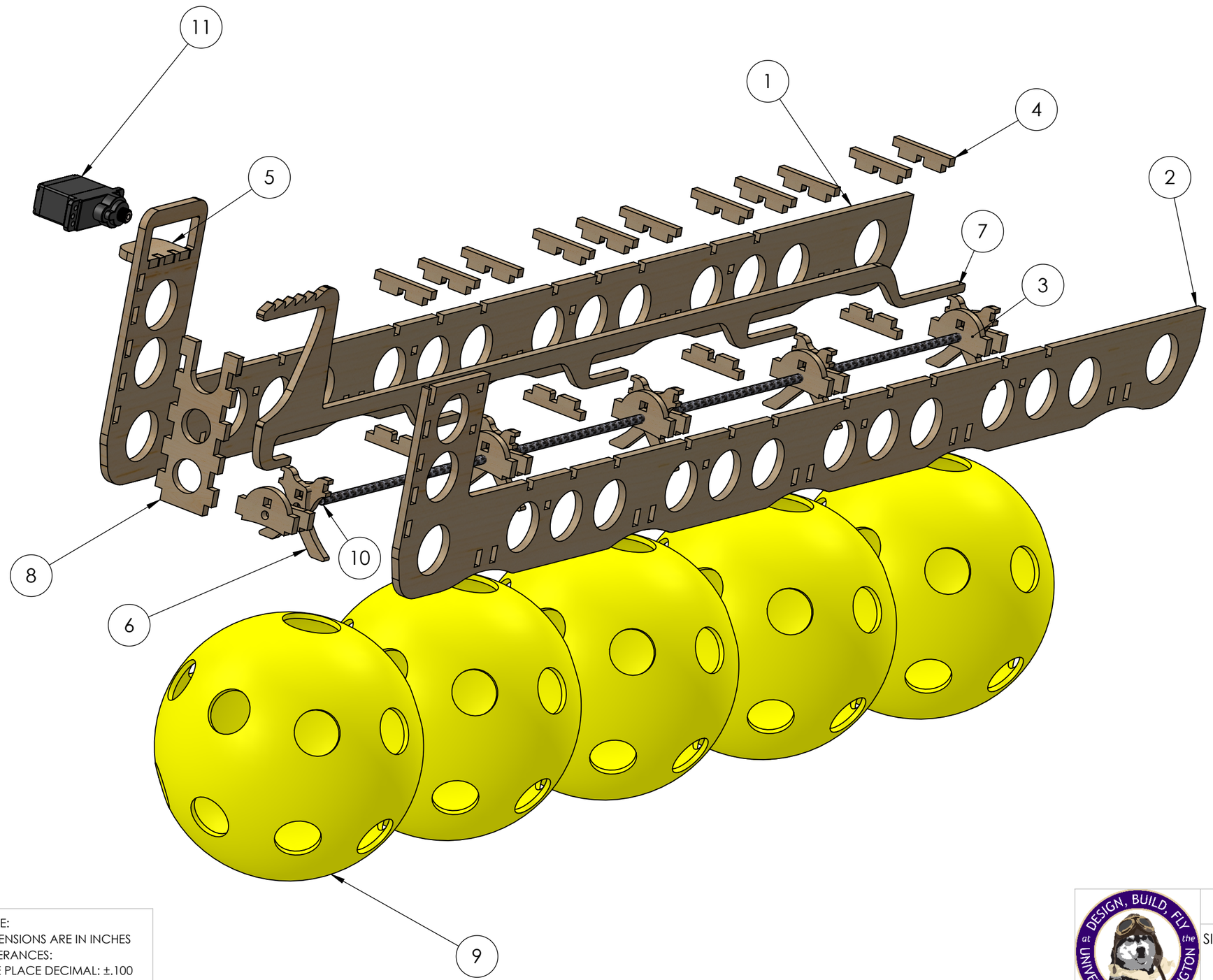

Number	DESCRIPTION	QTY.
1	Main Frame Right	1
2	Main Frame Left	1
3	Cross Frame	5
4	Top and Bottom Pin Guide	15
5	Servo Mount	1
6	Clip for Wiffle Ball	10
7	Main Pin	1
8	Brace for Main Frames	1
9	Wiffle Ball 12 Inch Diameter	5
10	Carbon Fiber Rod	1
11	Micro Servo HiTEC HS-5065 MG	1

NOTE:
DIMENSIONS ARE IN INCHES
TOLERANCES:
ONE PLACE DECIMAL: ±.100
TWO PLACE DECIMAL: ±.030
THREE PLACE DECIMAL: ±.005

University of Washington

CESSNA - RAYTHON - DESIGN BUILD AND FLY 2014-2015

SIZE B

TITLE: DROPPING MECHANISM

SCALE: 2:3

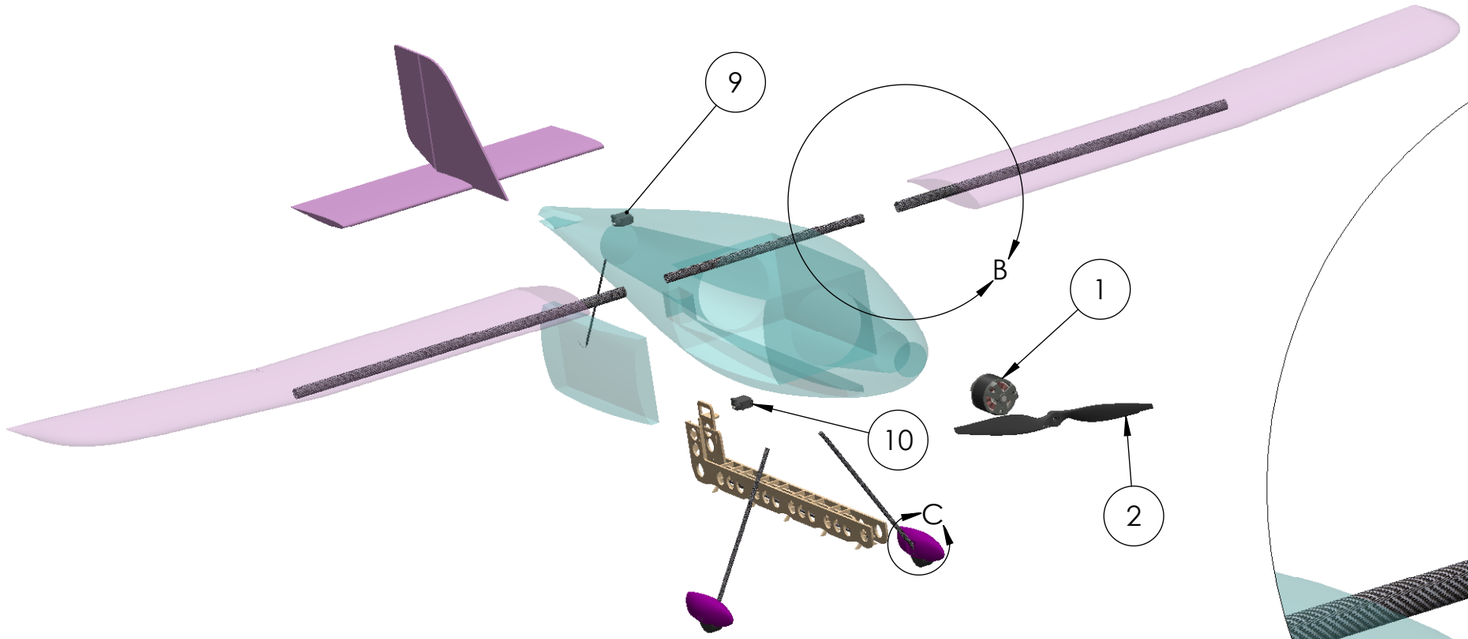

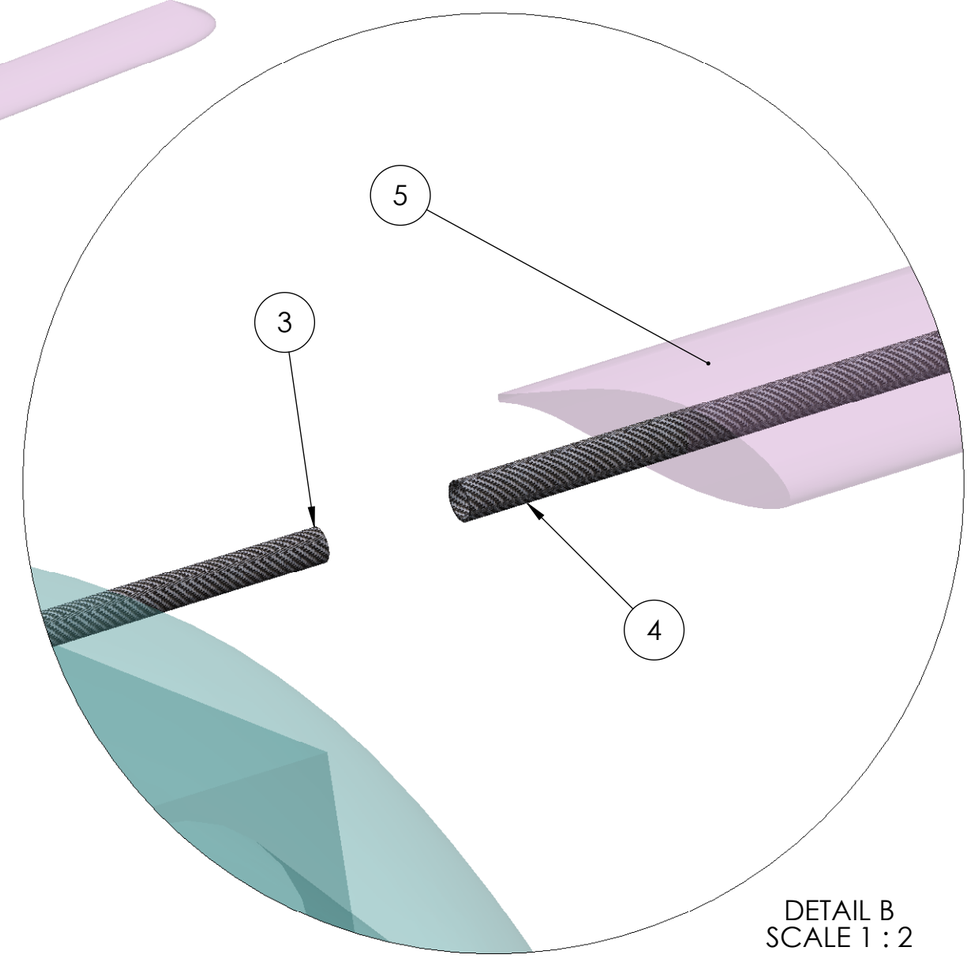

DETAIL B
SCALE 1 : 2

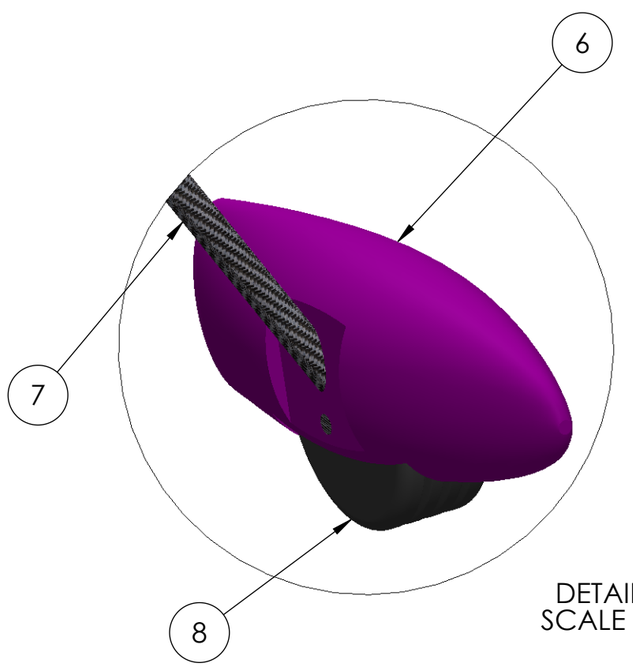

DETAIL C
SCALE 1 : 1

PRIMARY COMPONENTS	
1	ENGINE
2	PROPELLER
3	INNER SPAR FUSELAGE
4	OUTER SPAR WING
5	WING ASSEMBLY
6	3D PRINTED LANDING GEAR
7	LANDING GEAR STRUT
8	WHEEL
9	RUDDER SERVO
10	DROPPING MECHANISM AND ELEVETOR SERVO

NOTE:
DIMENSIONS ARE IN INCHES
TOLERANCES:
ONE PLACE DECIMAL: ±.100
TWO PLACE DECIMAL: ±.030
THREE PLACE DECIMAL: ±.005

University of Washington

CESSNA - RAYTHON - DESIGN BUILD AND FLY 2014-2015

SIZE B

TITLE: STRUCTURE LAYOUT

SCALE: 1:8

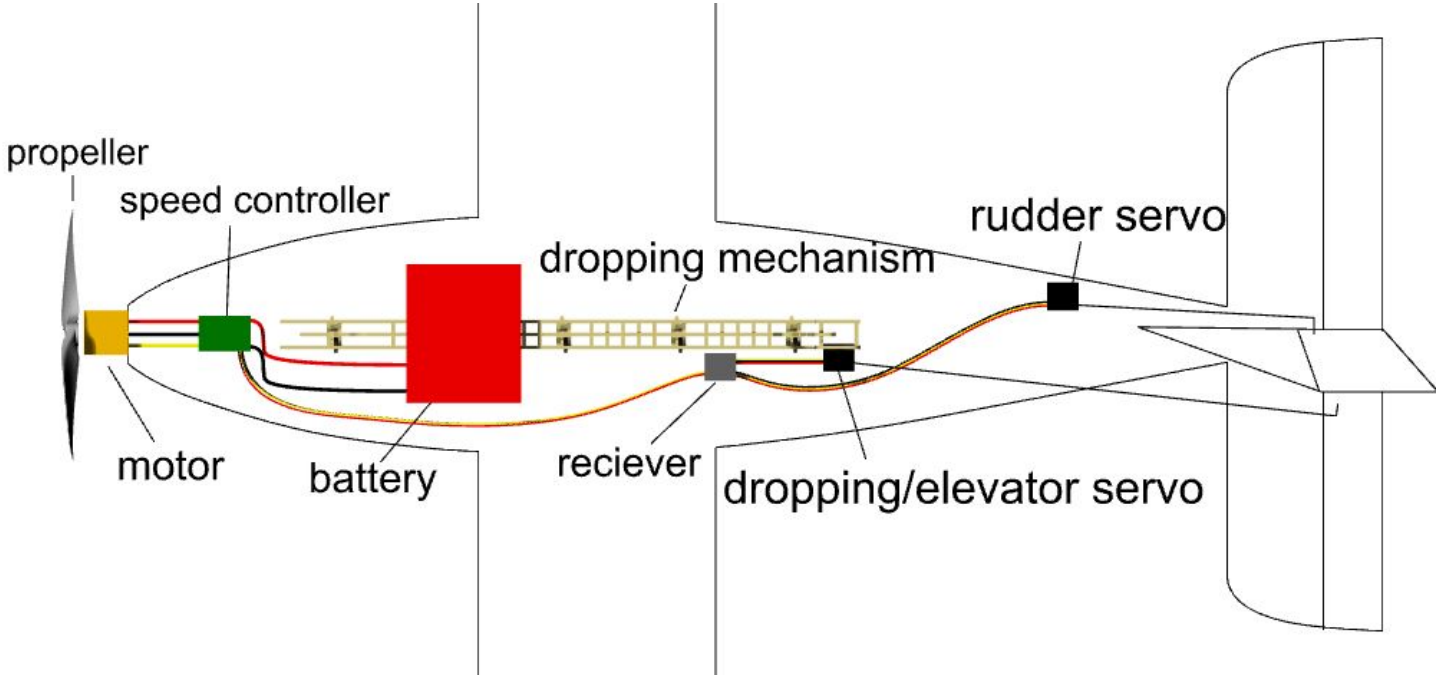
propeller
speed controller
dropping mechanism
rudder servo
motor
battery
reciever
dropping/elevator servo

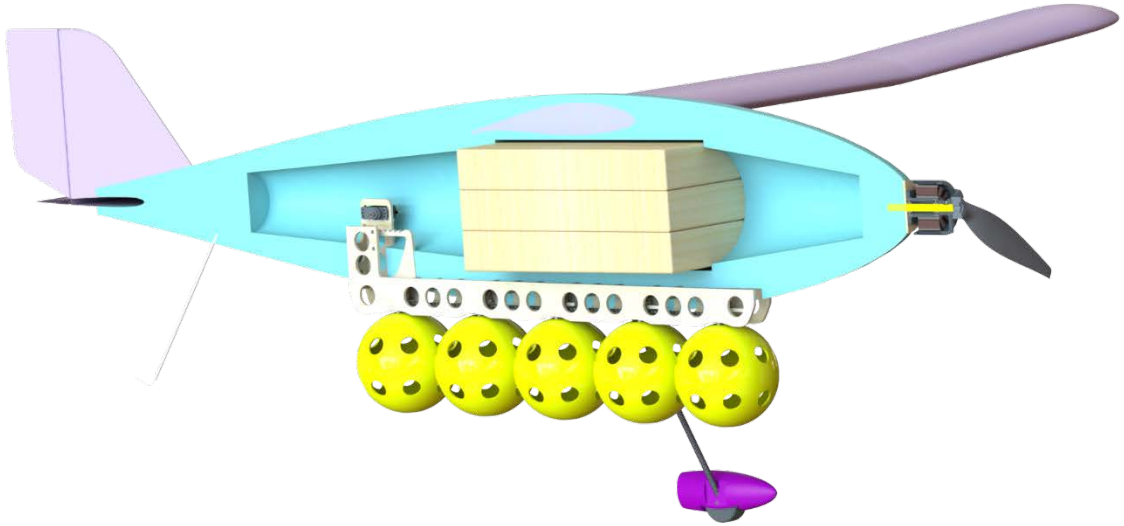

6. Manufacturing Plan

6.1 Manufacturing Schedule

Table 6.1 below displays the manufacturing schedule of the three prototypes and the final competition model. As shown, prototype 1 and 2 are currently finished, while prototype 3 and the final competition model will be built in the two months before the competition. Note that the time frame is not to scale, since the dates are not evenly assigned in the table.

Table 6.1: Manufacturing Schedule

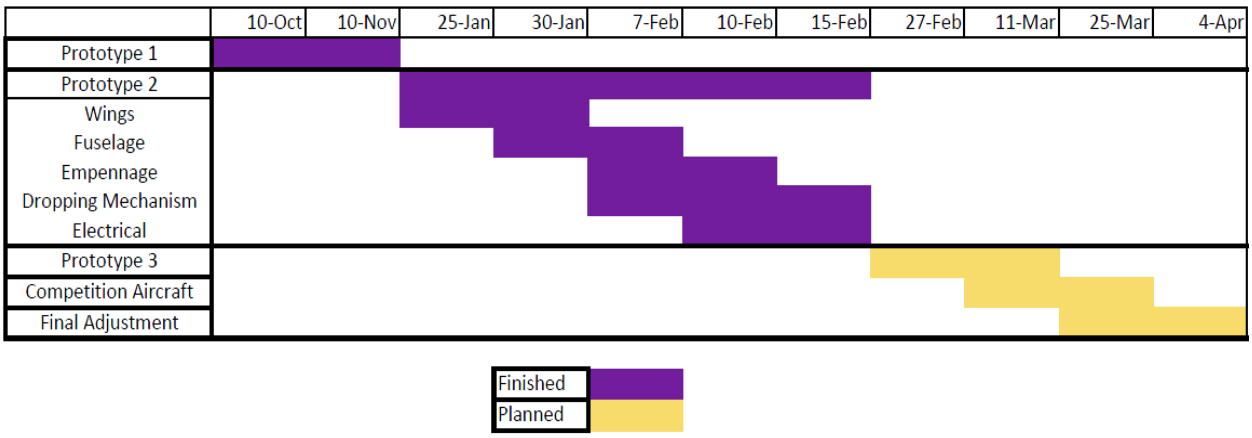

6.2 Material Selection

The team went through an extensive material selection process, and the tradeoff decisions are recorded in the following table.

Table 6.2: Material Selection Trade Table

	Location	Advantages	Disadvantages	Tradeoff Decisions
Composite (Carbon Fiber)	**fuselage, empennage, tail boom, landing gear**	**High strength to weight ratio**	**Hard to repair if damaged, more expensive**	**Because it is not used in large amounts, it is still the strongest and lightest material available.**
Foam	**Wings, fuselage**	**Lightweight, easy to craft, inexpensive**	**Not as strong as carbon fiber**	**Less labor-intensive than carbon fiber and lighter**
Plywood	**Dropping mechanism**	**Light weight, inexpensive, easily accessible**	**Not as strong as carbon fiber, heavy**	**Using competition balsa wood, half as heavy and equally strong as regular balsa wood**

6.3 Major Component Manufacturing Process

6.3.1 Wings

The wings were cut from Owens Corning pink insulation foam with a hot wire cutter. Because the team did not have access to a CNC wire cutter, laser-cut plywood guides were made for handheld wire. These guides consisted of a top and bottom portion of the airfoil, and incorporated a 1/16" trailing edge thickness for structural integrity. This is demonstrated in Figure 6.1.

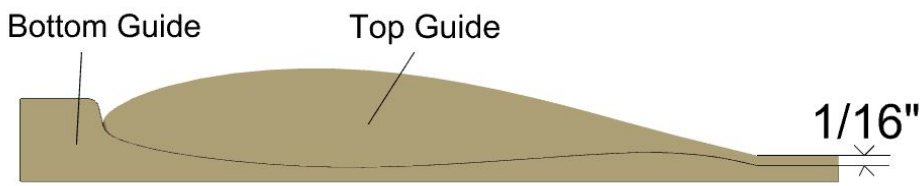

Figure 6.1: Laser-cut plywood guides used for airfoil fabrication

The hot wire was dragged along the top and bottom stencils until a complete airfoil had been cut from the precut foam block. Figure 6.2 shows this.

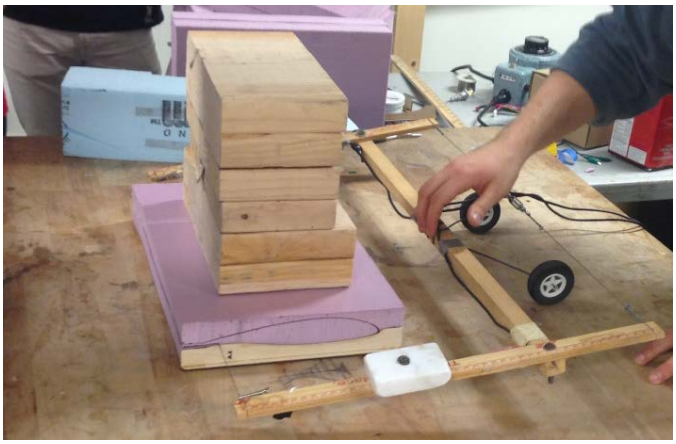

Figure 6.2: Airfoil fabrication

After the foam was cut, a channel was cut for the carbon fiber spars, which were then glued in place with epoxy. Once the carbon fiber was incorporated, the entire wing was laminated with Monokote and strapping tape to increase rigidity and reduce surface friction.

6.3.2 Fuselage

Because of the complex contours of the fuselage shape, and precision required in the dimensions, it was decided to use a CNC router to cut the fuselage, using DOW blue insulation foam. NX9, a CAD and CAM software, was used to generate the tool path for the mill. Each half, left and right, of the fuselage was milled and then post processed with sandpaper to increase smoothness. The fuselage at this step is shown in Figure 6.3. Once the fuselage halves were milled, the dropping mechanism, motor mount, wing-joining spar and landing gear mounts were all glued in place. At this point the entire fuselage was laminated in clear Monokote and strapping tape to increase rigidity and decrease surface friction. The horizontal and vertical tail were permanently glued to the rear of the fuselage, and laminated in Monokote.

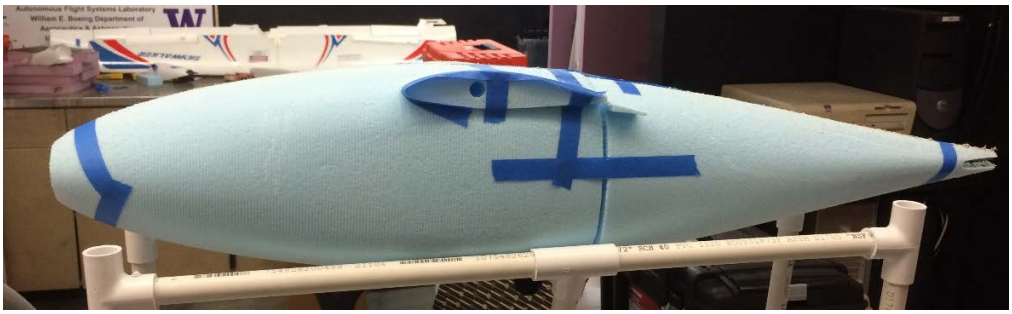

Figure 6.3: CNC-milled fuselage

6.3.3 Landing Gear

The landing gear was constructed mostly of carbon fiber tubes to reduce weight and increase resilience and strength. In order to mount the carbon axle to the carbon strut, the two pieces were glued together with cyanoacrylate, and the carbon fiber thread saturated in epoxy was wrapped around the joint. In order to mount the landing gear strut to the fuselage, a wooden block was shaped to conform to the fuselage side and a hole was drilled at an angle to house the carbon strut (Figure 6.4).

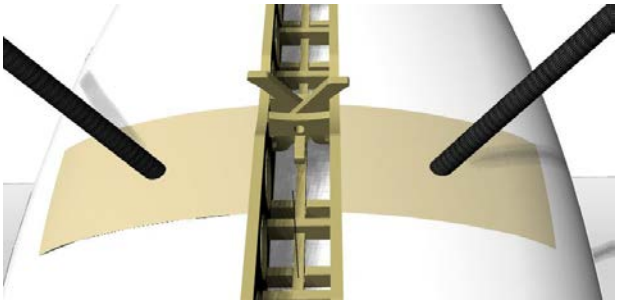

Figure 6.4: Landing gear struts attached to the fuselage

6.3.4 Dropping Mechanism

The dropping mechanism was designed to release the plastic balls individually with the elevator servo. This required a complex and precise structure. In order to meet the precision requirement, the team opted to laser cut the mechanism from plywood (Figure 6.5). This enabled a fast manufacturing time and a strong and light structure.

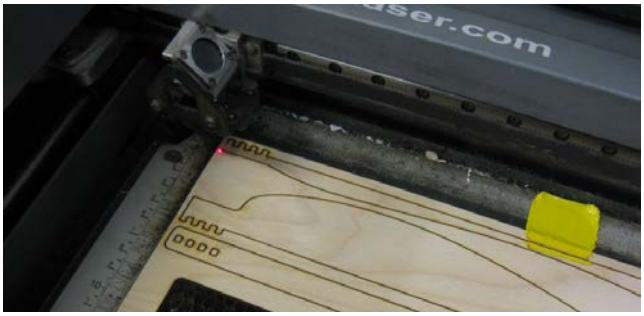

Figure 6.5: Laser cutting of the dropping mechanism

6.3.5 Motor and Servo Mounting

The motor mount is a simple 1/8” plywood disk which was glued the front of the fuselage. Fiber tape and packing tape was wrapped around the front of the mount to ensure a secure attachment to the fuselage.

Because the elevator servo actuates both the elevator and the dropping mechanism, it was mounted to the dropping mechanism structure (Figure 6.6). The rudder servo was mounted in the foam near the tail end of the fuselage (Figure 6.7).

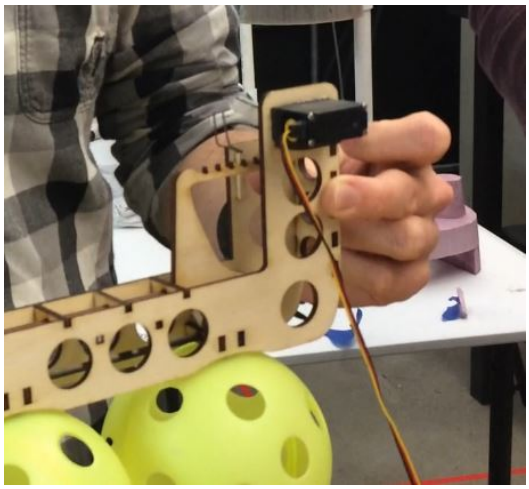

Figure 6.6: Elevator and dropping mechanism servo

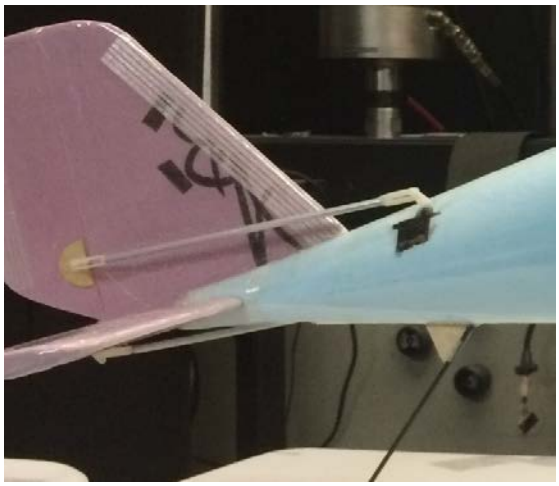

Figure 6.7: Rudder servo and linkage

7. Testing Plan

Subsystem tests were conducted in order to acquire performance data, which indicated the parts that were subject to improvement. Flight tests determined basic performance parameters of the aircraft and ensured the aircraft model was able to complete all the competition missions.

7.1 Subsystem Test

7.1.1 Battery Test

The main purpose of battery testing was to ensure the power is sufficient for the aircraft to complete every single mission. Thus, two battery endurance test were conducted in-flight: one with the aircraft empty, and another with the aircraft fully loaded. For each test, the aircraft took off with a fully charged battery and flew until the power cut out. The time duration was measured and compared with the time necessary to successfully complete the mission.

7.1.2 Propulsion System Test

Static thrust tests were performed on the motor and the propeller selected. During a static thrust test, shown in Figure 7.1, the propeller was mounted on an L-bracket which transferred the thrust produced by the propeller to a scale. The reading was then compared to the manufacturer's rated performance to ensure the propulsion system could achieve the expected performance.

Figure 7.1: Static thrust testing of the propeller

7.1.3 Structure Test

The wings and spar were tested for strength by propping the structural prototype between two level surfaces with only the tips of the wings on each surface as shown in Figure 7.2. Weights were then added onto the top of the aircraft body until the wing structure failed. The maximum load, wingtip deflection, and failure location were recorded for spars made of different materials, giving insight into which spar would be best for future prototypes and the final aircraft.

Figure 7.2: Structural testing of the wings

The strength of the landing gear was tested by pulling the landing gear in two different directions: upwards relative to the aircraft (Figure 7.3) and backwards relative to the aircraft (Figure 7.4). Pulling the landing gear in these two directions served to simulate the two load components that would be experienced at touchdown. Both components of the force experienced by the landing gear were tested until landing gear strut failure.

Figure 7.3: Landing gear strut testing in the backward direction

Figure 7.4: Landing gear strut testing in the upward direction

7.1.4 Loading and Unloading Test

These tests were performed to determine the performance of the aircraft during the ground mission. The payload of mission 2 was unloaded and then the external payload of mission 3 was installed as quickly as possible. The aircraft was loaded and unloaded multiple times, all while being timed in order to determine if the aircraft could be completely loaded and unloaded within 5 minutes. All of the connection joints were checked to see if they remained structurally sound.

7.2 Flight Test

7.2.1 Take-Off Test

The purpose of executing the take-off test was to ensure that the aircraft had sufficient power to take off within 60 feet without overloading the wings. The take-off distance with both empty load and maximum loaded aircraft were measured on the runway during the test and confirmed to fall well within the allowed limitations.

7.2.2 Flight Mission Simulation

The purpose of the mission simulation was to ensure that the aircraft is capable of completing all of the missions during the competition, as well as to ensure that the pilot has sufficient control over the aircraft. The number of laps for mission 1, the flight time for mission 2, and the number of successful laps for mission 3 were determined during the simulation. The field selected for the simulation was measured and marked prior to the simulation to match the specifications of the competition course. The average speed was calculated based on the distance that the aircraft traveled and the flight time. Before each simulated mission, the take-off weight was measured at the testing site.

7.2.3 Flight Log

For each flight, a comprehensive flight log was filled out with important data collected prior to takeoff, during flight, and after landing. A pre-flight checklist and a post-flight checklist was included in order to validate the airworthiness of the aircraft being flown. The format of the flight logs used can be seen in Figure 7.5.

Design, Build, Fly at the University of Washington Flight Log

Note: Please upload this flight log to the online folder pertaining to the corresponding aircraft.

Flight #: _____ Take-Off Time: _____:_____ AM / PM

Date of Flight: _____/_____/_____ Flight Duration: _____ Min _____ Sec

Battery Used: _____ CG Location: _____

Total Takeoff Weight: _____ lb. Weather: _____

Wind Conditions: _____ mph, coming in from N / NE / E / SE / S / SW / W / NW

Pre-Flight Checklist:

- o Motor securely fastened
- o Wing securely fastened
- o Empennage securely fastened
- o Landing gear lubricated and rolling smoothly
- o Payload onboard and secured
- o Main battery connected
- o Propeller free of obstructions
- o Power on
- o Full control surface deflection
- o Full motor speed control

Post-Flight Checklist:

- o Power off
- o Main battery disconnected
- o Aircraft inspected for damage

Purpose of Flight:

_____

_____

_____

Payload:

_____

_____

_____

Notes:

_____

_____

_____

_____

_____

Figure 7.5: Flight log format

7.3 Testing Schedule

Table 7.1 shows the date of major flight tests where the entire crew were present. Smaller scale flight tests were conducted multiple times weekly before the prototype was ready for a major flight test event. Smaller scale flight tests took place in the IMA field of University of Washington and major flight tests took place at Magnuson Park in Seattle, WA, or Marymoor Park in Redmond, WA.

Table 7.1: Major flight test dates, locations, and objectives

Date	Objectives
11/21/2014 (First Prototype)	This test verified the feasibility of the conceptual design and tests control system concepts. No payloads were flown.
02/18/2015 (Second Prototype)	This test simulated the entire mission and verifies the detailed aircraft design.
03/14/2015 (Planned) (Third Prototype)	This test will verify that the improvements made perform as expected. Mission simulation will again be conducted.
03/28/2015 (Planned) (Competition Model)	This test will test the capability of the competition-ready model. Adjustments will be determined.
04/04/2015 (Planned) (Competition Model)	This test will verify that the adjustments made meets the team's expectation. This test will also serves as a final practice run for the pilot.

8. Performance Results

8.1 Subsystem Test Results

8.1.1 Main Battery Test

The endurance of the main battery was tested by flying the aircraft at cruising speed and recording the time until the power cut off. The lasting time was measured for the maximum loaded aircraft, aircraft with externally loaded plastic balls, and the empty aircraft (Table 8.1).

Table 8.1: Battery endurance for empty and fully loaded aircraft

Empty Load	**12.7 min**
Maximum Load	**7.3 min**
With External Plastic Balls	**10.6 min**

Mission 1 requires the empty aircraft to fly at near full throttle for 4 min. As demonstrated in the endurance test, the battery and motor selected are capable of providing sufficient power for mission 1, with a safety factor of over 300%. Mission 2 requires the maximum loaded aircraft to fly 3 full laps. Since it only takes around 2 minutes for the maximum loaded aircraft to fly 3 full laps, as shown in the mission simulation result, a 7.3 min endurance can ensure the completion of mission 2. Since the aircraft can carry 5 plastic balls in total, the aircraft needs to complete five laps in order to drop one ball per lap. Referencing the simulated time to complete mission 3 in Table 8.X, the completion of mission 3 can also be ensured, with 10.6 minutes of battery endurance.

8.1.2 Propulsion System Test

The thrust that the designated combination of motor and battery can provide is shown to be 37.18 N according to the static thrust test. As analyzed in Section 4.3.6, the minimum thrust needed for the aircraft to take off is 17.1 N, which indicates the combination of motor and battery is capable of

completing the take-off. The result of the tested thrust also agrees with the performance output from the MATLAB code elaborated in Section 4.3.6.

8.1.3 Structure Test

During the wing and spar strength test, in which the whole aircraft was only supported on the wing tip and loaded until failure, the failure location is determined to be at the connection of the flat panel and the deflected panel of the polyhedral wing, and the maximum load the wing can bear is determined to be 24 lbs, which translates to 3G under the 8 lb. maximum loaded weight.

According to the structure test for the landing gear, the land gear can withstand 16 lb. before breaking upward and 10 lb. before breaking backward. With a conservative maximum loaded weight of 8 lb., this test indicates that the aircraft can survive up to a 2G impact on landing.

8.1.4 Loading and Unloading Test

During the loading and unloading test, the wood block payload of mission 2 can be easily installed and uninstalled, because the cabin inside the fuselage has a large enough clearance with the payload, and the side door opens and closes with minimal effort. However, it took a relatively long time for the team to install the payload for mission 3. Because the dropping mechanism is a simple structure with pin and latches, each plastic ball must to be installed separately to the dropping mechanism, and special tool is needed to manually open the latches to hold the plastic ball. It took the team 4 min to finish loading the payload for mission 2, secure the aircraft, unload the payload for mission 2, load the payload for mission 3, and secure the aircraft. The ground mission can still be completed within 5 min as required, but in order to achieve a higher score, fine-tuning of the dropping mechanism must be made, so that the latches can be easily accessed and opened.

8.2 Flight and Mission Performance

8.2.1 Take-off Test

During the take-off test, the take-off distance for both empty load and maximum load was measured and tabulated in Table 8.2 below:

Table 8.2: Take-off distance

Empty Load	**8 ft.**
Maximum Load	**20 ft.**

As shown in Fig. 8.1, the aircraft took off before the 60 ft. line (drawn in white on the runway).

Figure 8.1: Prototype 2 climbing on take-off at maximum load

8.2.2 Flight Mission Simulation

All flight missions were performed by the aircraft model in order during the second major flight test demonstrated in the test schedule in Section 7.3. Before each mission, the take-off weight is measured on site. The tested mission performance is recorded and compared to the expected mission performance, as shown in Table 8.3.

Table 8.3: Tested mission performance compared with expected mission performance

	Take-off Weight (lb.)	Scoring Parameters	Expected	Tested
Mission 1	2.6	Number of Laps	8	8
Mission 2	7.6	Flight Time	2.04 min	2.15 min
Mission 3	3.34	Number of Laps	5	5

Mission 1 and 3 were completed as expected, while for mission 2 it took longer for the aircraft to complete 3 laps than calculated due to the imperfect flight course.

The total mission score can be calculated based on the simulated mission performance and RAC. The total mission score that Design, Build, Fly at University of Washington received in the simulation is 4.54. The team believes the aircraft model has potential to be further optimized before the competition, and the final competition aircraft will be highly competitive in the 2014-2015 AIAA Design/Build/Fly Competition. With hard work and enthusiasm, the UW team is excited and prepared to compete in the DBF Competition this April.

References

[1] Space Needle at Sunset. Digital image. *Space Needle*. N.p., n.d. Web. 22 Feb. 2015. <http://www.spaceneedle.com/news/wp-content/uploads/2014/03/sunset1.jpg>.

[2] Anderson, John D. *Fundamentals of Aerodynamics*, 5th Edition, McGraw-Hill, Boston, 2011. Print.

[3] "UIUC Airfoil Data Site." *UIUC Applied Aerodynamics Group*. N.p., n.d. Web. 21 Feb. 2015. <http://m-selig.ae.illinois.edu/ads/coord_database.html>.